HHS Public Access

Author manuscript

Brain Behav Immun. Author manuscript; available in PMC 2020 October 01.

Published in final edited form as:

Brain Behav Immun. 2019 October ; 81: 374–387. doi:10.1016/j.bbi.2019.06.034.

Noradrenergic dysfunction accelerates LPS-elicited inflammation-related ascending sequential neurodegeneration and deficits in non-motor/motor functions

Sheng Song[1,4], **Qingshan Wang**[1,2], **Lulu Jiang**[1,3], **Esteban Oyarzabal**[1,4], **Natallia V. Riddick**[5], **Belinda Wilson**[1], **Sheryl S. Moy**[5], **Yen-Yu Ian Shih**[4], **Jau-Shyong Hong**[1]

[1]Neuropharmacology Section, Neurobiology Laboratory, National Institute of Environmental Health Sciences, National Institutes of Health, Research Triangle Park, North Carolina, USA

[2]Department of Toxicology, School of Public Health, Dalian Medical University, Dalian, Liaoning, China

[3]Institute of Toxicology, School of Public Health, Shandong University, Jinan, Shandong, China

[4]Biomedical Research Imaging Center, University of North Caroline at Chapel Hill, Chapel Hill, NC, USA

[5]Department of Psychiatry and Carolina Institute for Developmental Disabilities, University of North Carolina School of Medicine, Chapel Hill, NC 27599, USA

Abstract

The loss of central norepinephrine (NE) released by neurons of the locus coeruleus (LC) occurs with aging, and is thought to be an important factor in producing the many of the nonmotor symptoms and exacerbating the degenerative process in animal models of Parkinson's disease (PD). We hypothesize that selectively depleting noradrenergic LC neurons prior to the induction of chronic neuroinflammation may not only accelerate the rate of progressive neurodegeneration throughout the brain, but may exacerbate nonmotor and motor behavioral phenotypes that recapitulate symptoms of PD. For this reason, we used a "two-hit" mouse model whereby brain NE were initially depleted by DSP-4 one week prior to exposing mice to LPS. We found that pretreatment with DSP-4 potentiated LPS-induced sequential neurodegeneration in SNpc, hippocampus, and motor cortex, but not in VTA and caudate/putamen. Mechanistic study revealed that DSP-4 enhanced LPS-induced microglial activation and subsequently elevated neuronal oxidative stress in affected brain regions in a time-dependent pattern. To further characterize the effects of DSP-4 on non-motor and motor symptoms in the LPS model, physiological and

Correspondence to: Jau-Shyong Hong, Ph.D. hong3@niehs.nih.gov, P.O. Box 12233, Mail Drop F1-01, Research Triangle Park, North Carolina 27709, USA.

Conflict of interest

The authors declare they have no actual or potential competing financial interests.

Supplementary material

Supplementary material is available online.

behavioral tests were performed at different time points following injection. Consistent with the enhanced neurodegeneration, DSP-4 accelerated the progressive deficits of non-motor symptoms including hyposmia, constipation, anxiety, sociability, exaggerated startle response and impaired learning. Furthermore, notable decreases of motor functions, including decreased rotarod activity, grip strength, and gait disturbance, were observed in treated mice. In summary, our studies provided not only an accelerated "two-hit" PD model that recapitulates the features of sequential neuron loss and the progression of motor/non-motor symptoms of PD, but also revealed the critical role of early LC noradrenergic neuron damage in the pathogenesis of PD-like symptoms.

Keywords

Parkinson's diseases; progressive neurodegeneration; chronic neuroinflammation; locus coeruleus; norepinephrine; motor symptoms; nonmotor symptoms

1. Introduction

Parkinson's disease (PD) has traditionally been considered a motor movement disease. The pathological hallmark of PD is progressive neuronal loss in the dopaminergic (DA) substantia nigra pars compacta (SNpc) and the appearance of proteinaceous intracellular inclusions known as Lewy bodies (Dickson et al., 2009; Hoehn and Yahr, 1967; Litvan et al., 2003; Olanow and Tatton, 1999). The cardinal motor signs of PD become clinically evident when approximately 60% of SNpc neurons and 70%-80% of striatal dopamine content are lost (Fearnley and Lees, 1991). In addition to motor dysfunction, accumulating evidence indicates that PD patients also suffer from a wide range of non-motor symptoms, including hyposmia, gastrointestinal (GI) disturbances, anxiety, depression, and cognitive impairment, many of which are evident before the onset of motor disturbances (Braak et al., 2003; Langston, 2006).

Recent clinical and preclinical studies suggest that noradrenergic (NA) dysfunction in the locus coeruleus (LC) plays a critical role in the pathogenesis of PD (Richard et al., 2012). In PD patients, there is a caudo-rostral progression of neurodegeneration, in which neuronal loss is greater and earlier in the LC than nucleus basalis and SN (Braak et al., 2004; Braak et al., 2011; Zarow et al., 2003). The marked reduction of norepinephrine (NE) is found throughout the brain, a change that also occurs earlier than the loss of striatal dopamine (Rommelfanger et al., 2007). This raises intriguing questions about the NA system as a morphological marker and a potential target for therapeutic intervention, specifically targeting pre-motor symptoms, which usually occur 10-20 years prior to the clinical onset of PD (Hawkes et al., 2010).

Currently, the progress of research on the pathogenesis of PD non-motor symptoms and sequential neuronal loss has been hampered due to the lack of suitable animal models. Conventional neurotoxins such as MPTP and 6-hydroxydopamine used in acute PD models causes a rapid death of dopamine neurons, thereby limiting the experimental duration needed to study disease progression and emergence of non-motor symptoms. It has been reported that endotoxin is an environmental factor in the cause of PD (Niehaus and Lange, 2003). Moreover, our recent study revealed a caudo-rostral progression of neurodegeneration

in LPS-injected mouse (Song et al., 2018). This neuroinflammatory model recapitulates the delayed and progressive motor deficits and DA neurodegeneration (Block et al., 2007; Qin et al., 2007), however, its relevance to PD-like non-motor symptoms remain undefined.

We have reported that NE has potent anti-inflammatory/neuroprotective properties in the central nervous system (Jiang et al., 2015). Given the wide projection of LC-NA neurons to almost the entire brain and their important role in regulating non-motor behaviors, we hypothesized that prior damage of LC-NA neurons may render neurons in LC-NA innervated regions more vulnerable to inflammation-mediated neurodegeneration and accelerate the appearance of both non-motor and motor symptoms. To test this possibility, we depleted mouse NE by using a selective NA neurotoxin N-(2-chloroethyl)-N-ethyl-2-bromobenzylamine (DSP-4) (Fritschy and Grzanna, 1989; Jonsson et al., 1981; Ross and Renyl, 1976), followed by a systemic injection of LPS. We found DSP-4 greatly enhanced LPS-induced microglial activation and sequential neuronal loss in all LC-NA innervated regions and accelerated the appearance of non-motor/motor symptoms in this combined toxin model. This study provides a novel “two-hit” mouse model that closely mimics human sequential and progressive neuronal loss and non-motor/motor manifestations of PD, and a window of opportunity for screening neuroprotective interventions.

2. Materials and Methods

2.1. Animals and treatment

Male C57BL/6J mice were obtained from the Jackson Laboratory (Bar Harbor, ME). Housing and breeding of animals were performed humanely with regard for alleviation of suffering following the National Institutes of Health’s Guide for the Care and Use of Laboratory Animals (Institute of Laboratory Animal Resources, 2011). A single systemic injection of DSP-4 (50 mg/kg, i.p.; Sigma-Aldrich, St. Louis, MO) or vehicle (saline, 5 ml/kg, i.p.) was administered to 9-week old male C57BL/6 mice (9-14 weeks of age for the second batch of animals) to deplete NE in the brain. One week later, LPS (15×10^6 EU/kg, i.p.; Sigma-Aldrich, L3012, St. Louis, MO) or vehicle was injected to both groups to induce chronic neuroinflammation. LD50 of LPS in these mice is around 25-30 mg/kg, which equals $5x10^7$ - $6x10^7$ EU/kg (Li et al., 2018). Since the potency of LPS varies from lot to lot even with the same catalog number, we used EU/kg as a dose unit of LPS is more accurate and consistent than mg/kg. We dosed two batches of animals for behavioral tests. The first batch of animals was evaluated for both non-motor and motor symptoms along with histological changes in different brain regions within a one-year time duration. The second batch of animals was used to further characterize non-motor symptoms in our “two-hit” mouse model, with the duration of behavioral tests extended to 21 months, since the first batch had been sacrificed for histological studies. The body weight was monitored twice per week.

Mice were housed on a 12 h:12 h light:dark schedule with lights on at 7 AM. All behavioral testing was conducted during the light phase of the light/dark cycle. All the experimental mice are transferred to the behavior testing room 30 min prior to beginning the first trial to habituate to the condition of the behavior testing room. Testing was conducted under fluorescent laboratory lighting (180-205 1x for the Morris water maze; 320-340 1x for

elevated plus maze and 3-chamber social choice test). All procedures were approved by the National Institutes of Environmental Health Sciences Animal Care and Use Committee.

2.2. Immunohistochemistry

Mice were euthanized using fatal plus at the desired time points after injection. Under deep anesthesia, mice were rapidly transcardially perfused with 15ml of ice-cold 1X PBS containing heparin for approximately 2 miniutes, followed by perfusion with ice-cold 4% paraformaldehyde (PFA; 25 ml at 5 ml/min). Brains were further post-fixed in 4% PFA for 24 hours, then transferred to ice-cold 10% sucrose solution and incubated at 4°C overnight. The 10% sucrose were then replaced with ice-cold 30% sucrose, and brains were allowed to equilibrate completely at 4 °C, as evidenced by their sinking to the bottom of the container. Brains were then sectioned immediately on a freezing sliding microtome and processed for immune-staining as described previously (Wang et al., 2014; Wang et al., 2015). We used the following primary antibodies for immunohistochemistry: antibodies against tyrosine hydroxylase (TH, rabbit: AB152, 1:4000; EMD Millipore, Temecula, CA), neuronal nuclei (Neu-N, 1:4000, CHEMICON, Temecula, CA), ionized calcium binding adaptor molecule-1 (Iba-1; 1:5000, Wako Chemicals, Richmond, VA), and CD11b (1:400, AbD Serotec, Raleigh, NC). Immuno-staining was visualized by using 3,3′-diaminobenzidine (DAB) and urea-hydrogen peroxide tablets or nickel-enhanced DAB.

2.3. Cell counts

2.3.1. Stereological counting assessments of neurodegeneration.—

Free-floating 35 μm coronal sections containing the SNpc, VTA, hippocampus, motor cortex and caudate/putamen (CPu) were cut on a horizontal sliding microtome. A total of 8 sections were sampled at 105 μm intervals for each brain region. Dopaminergic neurons of the VTA and SNpc were identified through TH^+ immunohistochemistry, whereas the pan-neuronal marker NeuN was used to identify all neurons in the hippocampus, motor cortex and CPu. Stereological counts of TH^+ VTA and SNpc neurons were estimated using an optical fractionator method on an Olympus BX50 stereological microscope within user-defined boundaries (Song et al., 2018; Wang et al., 2014; Wang et al., 2015). Briefly, systematic random sampling of sites with an unbiased counting frame (100 μm × 100 μm) within defined boundaries of the SN was performed. An 11 μm dissector height was used, and the guard zone was set at 2 μm. The counts were conducted with an Olympus BX50 microscope using a 60× 1.4NA oil immersion objective, and the coefficient of error values were less than 0.1.

2.3.2. Automated counting of single color images.—

The number of NeuN positive neurons in the hippocampus granule layer, motor cortex and CPu was measured by automated counting of single color images using ImageJ software (Cai et al., 2011). This method was based on the protocol created by Christine Labno (University of Chicago, Integrated Light Microscopy Core). Briefly, the color images were converted into gray scale, and then the threshold of the image was adjusted to highlight all the structures to be counted. After using the Binary Watershed to separate the merged particles, the total number of cells was analyzed (with the size of the target particles adjusted to avoid the “noise” pixels). The threshold of the image and the size of the counted particles were kept consistent among all

the images. All immunohistochemistry images were captured by a Leica Aperio AT2 Scanner.

2.4. Quantification of the immunohistochemistry staining density

The quantification of Iba-1 or CD11b immunohistological staining in SN, VTA, CPu, hippocampus, and motor cortex was performed by Image J software based on a protocol for quantifying western blots (Gassmann et al., 2009). Briefly, the image was first converted into the grayscale picture, and the background was adjusted before the quantifying area was selected for the measurement of the total pixels. The relative density of the staining was compared based on the density of the total pixels of a certain brain region (total pixels/area).

2.5. Confocal double-label immunofluorescence

The free-floating sections were immune-blocked with 4% goat serum in 0.25% triton/PBS for 2 hours and then incubated with 3-Nitrotyrosine (3-NT, mouse, 1:200, Abcam, Cambridge, MA), 4-Hydroxynonenal (4-HNE, rabbit, 1:200, Abcam, Cambridge, MA) or $gp91^{phox}$ antibody (mouse, 1:500, BD Biosciences, 611414) antibodies overnight at 4 °C. On the second day, the sections were washed with 1% BSA in 0.25% triton/PBS before incubation with polyclonal rabbit anti-TH antibody (mouse: MAB318, 1:2000; rabbit: AB152, 1:2000; EMD Millipore, Temecula, CA) overnight at 4 °C. The double-label immunofluorescence pictures were taken under the confocal microscope using Alexa-488 (green) and Alexa-594 (red) conjugated secondary antibodies (1:1,000) to visualize the double TH and 3-NT, 4-HNE or $gp91^{phox}$-positive neurons. Densitometry was performed using ImageJ.

2.6. One-hour stool collection

Each mouse was placed in a separate clean cage and observed throughout the 60 min collection period. Fecal pellets were collected immediately after expulsion and placed in sealed (to avoid evaporation) 1.5 ml tubes. Tubes were weighed to obtain the wet weight of the stool; this was then dried overnight at 65°C and reweighed to obtain the dry weight (Li et al., 2006).

2.7. Buried food test for olfactory function

Several days before the olfactory test, an unfamiliar food (Froot Loops, Kellogg Co., Battle Creek, MI) was placed overnight in the home cages of the mice. Observations of consumption were taken to ensure that the novel food was palatable. Sixteen to twenty hours before the test, all food was removed from the home cage. On the day of the test, each mouse was placed in a large, clean tub cage (46 cm L × 23.5 cm W × 20 cm H), containing paper chip bedding (3 cm deep), and allowed to explore for five minutes. The mouse was removed from the cage, and one Froot Loop was buried in the cage bedding. The mouse was then returned to the cage and given fifteen minutes to locate the buried food. Measures were taken of latency to find the food reward.

2.8. Elevated plus maze

This test was used to assess anxiety-like behavior, based on a natural tendency of mice to actively explore a new environment, versus a fear of being in an open area. Mice were given one five-minute trial on the plus maze, which had two walled arms (the closed arms, 20 cm in height) and two open arms. The maze was elevated 50 cm from the floor, and the arms were 30 cm long. Mice were placed on the center section (8 cm × 8 cm) and allowed to freely explore the maze. Measures were taken of time on, and number of entries into, the open and closed arms.

2.9. Social approach in a 3-chamber choice test

Mice were evaluated for the effects of DSP-4 and/or LPS on social preference. The procedure consisted of 3 x 10-minute phases: a habituation period, a test for sociability, and a test for social novelty preference. The interphase duration between each phase was approximately 1 minute, the time needed to place one or both of the stranger mice into Plexiglas cages in the side chambers. The test mouse was confined to the center chamber during these two interphase periods. For the sociability assay, mice were given a choice between proximity to an unfamiliar male C57BL/6J adult mouse (stranger 1), versus being alone. In the social novelty phase, mice were given a choice between the already-investigated stranger 1, versus a new unfamiliar mouse (stranger 2). The social testing apparatus was a rectangular, 3-chambered box fabricated from clear Plexiglas. Dividing walls had doorways allowing access into each chamber. An automated image tracking system (Noldus Ethovision) provided measures of time spent in proximity to each cage and entries into each side of the social test box.

2.10. Acoustic startle/prepulse inhibition (PPI)

Measures were taken of the reflexive whole-body flinch, or startle response, following exposure to a sudden noise. Mice were tested with a San Diego Instruments SR-Lab system. Briefly, mice were placed in a small Plexiglas cylinder within a larger, sound-attenuating chamber (San Diego Instruments). The cylinder was seated upon a piezoelectric transducer, which allowed vibrations to be quantified and displayed on a computer. The chamber included a ceiling light, fan, and a loudspeaker for the acoustic stimuli (bursts of white noise). Background sound levels (70 dB) and calibration of the acoustic stimuli were confirmed with a digital sound level meter (San Diego Instruments). Each test session consisted of 42 trials, presented following a 5-min habituation period. There were 7 different types of trials: the no-stimulus trials, trials with the acoustic startle stimulus (40 ms; 120 dB) alone, and trials in which a prepulse stimulus (20 ms; either 74, 78, 82, 86, or 90 dB) had onset 100 ms before the onset of the startle stimulus. The different trial types were presented in blocks of 7, in randomized order within each block, with an average intertrial interval of 15 seconds (range: 10 to 20 sec). Measures were taken of the startle amplitude for each trial, defined as the peak response during a 65-msec sampling window that began with the onset of the startle stimulus. Levels of PPI (prepulse inhibition) at each prepulse sound level were calculated as 100 - [(response amplitude for prepulse stimulus and startle stimulus together / response amplitude for startle stimulus alone) × 100].

2.11. Morris water maze

2.11.1. Visible platform test.—The Morris water maze task was used to assess spatial learning. The maze consisted of a large circular pool (diameter=122 cm) partially filled with water (45 cm deep, 24-26°C), located in a room with numerous visual cues. Mice were first tested using a visible platform. In this case, each animal was given four trials per day, across two days, to swim to an escape platform cued by a patterned cylinder extending above the surface of the water. For each trial, the mouse was placed in the pool at one of four possible locations (randomly ordered), and then given 60 seconds to find the visible platform. If the mouse found the platform, the trial ended, and the animal was allowed to remain on the platform 10 seconds before the next trial began. If the platform was not found, the mouse was placed on the platform for 10 seconds, and then given the next trial. Measures were taken of latency to find the platform via an automated tracking system (Noldus Ethovision).

2.11.2. Hidden platform test.—Following the visual cue task, mice were trained to find a submerged, hidden escape platform (diameter=12 cm). As in the procedure for visual cue learning, each animal was given four trials per day, with one minute per trial, to swim to the hidden platform. Following five days of training, mice were given a one-minute probe trial in the pool with the platform removed. Selective quadrant search was evaluated by measuring time spent in the quadrant where the platform (the target) had been placed during training, versus time in the other three quadrants.

2.12. Accelerated Rotarod test

The accelerated Rotarod behavioral test was measured using a Rotamex device (Columbus Instruments). The parameters of the rotarod system include start speed, acceleration, and highest speed (1 rpm, accelerate 1 rpm/12 s, 50 rpm). In order to reach a stable performance, all mice were trained on the rotarod. The training was performed on three consecutive days before the first test. On the test day, accelerating rotarod was performed. The mice underwent three consecutive trials. The rest period between each trial was 30 min. The mean latency time to fall off the rotating rod for the last two trials was used for the analysis.

2.13. Wire hang test

The neuromuscular strength was determined by wire hang test. Each mouse was placed on a wire lid of a conventional housing cage, which was then inverted and suspended above the home cage; the latency to when the animal fell was recorded. This test was performed three times per time point with three trials per session. The average performance for each session was presented as the average of the trials.

2.14. Gait analysis

2.14.1. Forced gait analysis.—The forced gait analysis was performed using the DigiGait™ system (Mouse Specifics Inc., Boston, MA). Briefly, mice were placed on a transparent motor-driven treadmill belt and the gait was recorded with a high-speed digital video camera placed below the belt at a speed of 25 cm/s. The collected images were analyzed with the specific DigiGait Software 9.0 (Mouse Specifics, Quincy, MA) and

relevant gait parameters including stride length, stride variability and step angle were assessed.

2.14.2. Freely walking gait analysis.—To obtain footprints, the hind- and forefeet of the mice were coated with purple and orange nontoxic paints, respectively. The animals were then allowed to walk along a 50-cm-long, 10-cm-wide runway (with 10-cm-high walls) into an enclosed box. All mice had three training runs and were then given one run per week. A fresh sheet of white paper was placed on the floor of the runway for each run. The footprint patterns were analyzed for four step parameters (all measured in centimeters). Stride length was measured as the average distance of forward movement between each stride. For each step parameter, three values were measured from each run, excluding footprints made at the beginning and end of the run where the animal was initiating and finishing movement, respectively. The mean value of each set of three values was used in subsequent analysis.

2.15. Statistical analysis

All data are reported as means ± SEM. GraphPad Prism 8 (GraphPad Software, La Jolla, CA) was used for statistical analyses. In behavioral tests, data were collected by an experimenter blinded to treatment. To assess the effect of different treatments and time points on neuronal loss (Fig. 1B and 1D), microglial activation (Fig. 2), oxidative stress (Fig. 3), defecatory dysfunction (Fig. 6), Rotarod, Wire hang and DigiGait test (Fig. 10 A–D), two-way Analysis of Variance (ANOVA) followed by post hoc Tukey multiple comparison test was performed. The neuronal loss in Fig. 1C were performed by one-way ANOVA for each region with time as main effect, followed by post hoc Tukey multiple comparison test. The stride length of right forepaws (Fig. 10D) was analyzed using ordinary on-way ANOVA followed by post hoc Tukey multiple comparison test. Behavioral results from sociability test (Fig.4), Morris water maze test (Fig. 5), startle response test (Fig. 7), elevated plus maze test (Fig. 8), and olfactory test (Fig. 9) were analyzed using repeated measures ANOVA. Fisher's protected least-significant difference (PLSD) tests were used for comparing group means only when a significant F value was determined in the overall ANOVA. Within-group repeated measures analyses were used to determine side preference in the social approach test, and quadrant preference in the Morris water maze. For all comparisons, significance was set at adjusted $p < 0.05$.

3. Results

3.1. Pathological changes in "two-hit" mouse brain

We previously demonstrated that a single injection of LPS or DSP-4 in mice produces almost identical Parkinsonian-like neurodegeneration of DA-SNpc neurons with motor deficits at 10 months after injection (Song et al., 2018). To further characterize the pathological changes in "two-hit" mice, brains were evaluated for neurodegeneration, microglial activation, and oxidative stress.

3.1.1. DSP-4 treatment accelerates LPS-induced neuron loss in the NA neuron-innervated brain regions—Mice received a single systemic injection of DSP-4 (first treatment, 50 mg/kg; i.p.), a selective NA neurotoxin one week before LPS dosing

(second treatment, 15×10^6 EU/kg; i.p.), followed by examination of the neuronal loss in different brain regions at different time points (Fig. 1A). Results showed a significantly increase in neuronal loss in SNpc (25±7.5%) 3 months after "two-hit" treatment, while both DSP-4 and LPS alone failed to induce neuronal loss in SNpc (Fig. 1B, Supplementary Fig. 1A and C). LPS-induced neuronal loss was aggravated by DSP-4 in SNpc (37.5±5.5%) and the occurrence of neuronal loss was also observed in hippocampus (22.3±5.2%) and motor cortex (15±4.6%) regions 6 months after "two-hit" treatment (Fig. 1C–E). It is worth noting that, both DSP-4 alone and LPS alone mice show a delayed DA neuron loss at 6 months after injection, DSP-4 significantly potentiated LPS-induced DA neuron loss (Fig. 1B and D). However, in comparison to DSP-4 or LPS alone group, no significant synergistic toxicity was observed in SNpc (Fig. 1B) in "two-hit" mice, with a loss of 49±7.1% neurons, at 10 months after injection. Meanwhile, the synergistic toxicity of LPS by DSP-4 was also not found in hippocampus and motor cortex (Supplementary Fig. 1B and D) at 10 months, where there was a loss of 31.8±6.9% and 27.9±6.7% neurons, respectively. The loss of Neu-N^+ cell in hippocampal granular layer in Fig. 1E was further confirmed by hematoxylin staining in 5 μm paraffine-embedded sections (Supplementary Fig. 2A).

Interestingly, the regionally selective neurodegeneration was consistent with clinical evidence in PD patients, where no neurodegeneration was observed in two regions: caudate/putamen (CPu) and VTA, which are closely related to SN (Fig 1C and E, and Supplementary Fig. 1). The high-power images also showed very comparable Neu-N staining in CPu in all groups, while the decrease in Neu-N positive staining was found in motor cortex of DSP-4 alone, LPS alone, and "two-hit" animals (Supplementary Fig. 2A). Although no changes in VTA THir cells was found in the experimental animals, a significant decrease of neurites in SN reticulata (SNr) and VTA was observed in all toxin-treated animals (Supplementary Fig. 2B). Collectively, these results suggest that DSP-4 treatment potentiated not only LPS-induced neurodegeneration in LC/NE-innervated brain regions in our inflammation-mediated mouse model, but also exhibited a progressive and caudo-rostral pattern.

3.1.2. DSP-4 treatment potentiates LPS-induced microglial activation in the NA neuron-innervated brain—Chronic microglial activation is essential for inflammation-mediated neurotoxicity of dopaminergic neurons (Block et al., 2007; Qin et al., 2007). We previously reported that the release of NE in the SN region can exert a protective effect on DA neurons from LPS-elicited neuroinflammatory damage, which is dependent on the presence of microglia (Jiang et al., 2015). To explore if the synergistic toxicity of DSP-4 on LPS-induced inflammatory mouse model is associated with microglial activation, we used immunocytochemistry to measure CD11b and Iba-1, two microglia markers whose elevated expression is associated with microglial activation. Results showed that 6 months after DSP-4 alone or LPS alone treatment, microglia were significantly activated in SN, which was characterized by intensified CD11b (Fig. 2A–C) and Iba-1 staining (Fig. 2C–D) and hypertrophied morphology (Fig. 2C–D). The chronic and low-grade microglial activation was also found in SN, hippocampus and motor cortex at 3 months after DSP-4/LPS injection, and was sustained up to 10 months (Supplementary Fig. 3). However, LPS-induced microglial activation was markedly potentiated by DSP-4 in all these noradrenergic-innervated brain regions only at the early timepoints. Compared to the

LPS alone group, DSP-4 combined with LPS injection resulted in 128±5.1% ($^{\#}p<0.05$), 112±9.2%, and 111± 9.0% increase of CD11b density in SN, hippocampus, and motor cortex at 3 months after treatment (Supplementary Fig. 3A and C), which was elevated to 129±5.2% ($^{\#}p<0.05$), 131±11.0% ($^{\#}p<0.05$), and 146±6.0% ($^{\#}p<0.05$) at 6 months (Fig. 2A–B) and reduced to 110±14.2%, 116±30.3%, and 118±20.1% at 10 months (Supplementary Fig. 3B and D). Although DSP-4-, LPS- and "two-hit"-induced microglial activation was time-dependently increased in affected regions, no obvious synergetic microglial activation was found in all the regions in "two-hit" mouse brains at 10 months after treatment, indicating a saturated stable plateau.

However, as no changes in neuron loss were found in CPu and VTA, microglia in these two regions also remained unchanged in all the groups (Fig. 2A–B and Supplementary Fig. 3).

3.1.3. NE deficiency accelerates neuronal oxidative stress in "two-hit" mouse brains—Oxidative stress plays a central role in nigral DA neurodegeneration in PD patients and animal models (Dias et al., 2013). One of the major sources of superoxide in the brain is activated microglia, with most superoxide being produced by NADPH oxidase (Block et al., 2007). Since NE can inhibit NOX2 activation, we therefore measured oxidative stress in LC/NE-innervated brain regions to further explore the mechanism of caudo-rostral neurodegeneration. To this end, we quantified the levels of two products of oxidative stress, the 3-nitrotyrosine (3-NT) and 4-hydroxynonenal (4-HNE). Immunofluorescence analysis showed a clear increase in neuronal 3-NT and 4-HNE staining in SNpc at 6 months after DSP-4 or LPS injection (Fig. 3A–B), as evidenced by TH and 3-NT/4-HNE double immunolabeling (Fig. 3C). In addition, DSP-4 drastically enhanced LPS-induced neuronal oxidative stress in SNpc in a time-dependent manner: 3NT and 4-HNE (Fig. 3A–B). Furthermore, the increase of $gp91^{phox}$ staining, a key subunit of NADPH oxidase, also showed the same staining pattern as 3-NT/4-HNE after the injection of all toxins (Fig. 3D). Meanwhile, the double immunolabeling studies demonstrated that $gp91^{phox}$ immunoreactivity appeared to co-localize with Iba-1-positive cells (Fig. 3E and F). In addition to SN, the increased oxidative stress was also found in all those LC-innervated regions, such as CA1, DG, and motor cortex (Supplementary Fig. 4). Moreover, the striatal oxidative stress remains unchanged in all groups. Altogether, these results suggest that DSP-4 time-dependently potentiated LPS-induced neuronal oxidative stress in SN in a progressive manner.

3.2. DSP-4 treatment accelerates the appearance of non-motor symptoms in LPS-treated mice: Phenotypes in younger mice (4.5-12 months of age)

To determine whether DSP-4-enhanced caudo-rostral neurodegeneration in the different brain regions is associated with the appearance of non-motor symptoms, mice were assessed in non-motor behavioral tests at different ages. Mice were given the first treatment (either vehicle or DSP-4) at 9 weeks of age, and the second treatment (either vehicle or LPS) at 10 weeks of age. Mice were then tested in an elevated plus maze (no statistically significant difference, data not shown), acoustic startle procedure, social approach assay, buried food assay (no statistically significant difference, data not shown), and the Morris water maze. These results showed that, before one year of age, treatments showed no effects on

performance in the elevated plus maze or olfactory tests. However, as described below, exposure to DSP-4 and LPS led to significant changes in social preference, spatial learning, defecatory function, and startle response. There were no differences in body weight between treated groups vs. controls during these studies (Supplementary Fig. 5).

3.2.1. Loss of sociability in mice at 3.5 months after exposed to both DSP-4 and LPS—The three-chamber test can serve as a tool to identify deficits in sociability and/or social novelty in rodent models of CNS disorders. Under normal circumstances, rodents prefer to spend more time with another rodent (sociability) and will investigate a novel intruder more so than a familiar one (preference for social novelty). As shown in Fig. 4A, at 3.5 months after injections, mice treated with vehicle, DSP-4 alone, or LPS alone demonstrated robust preference for spending more time in proximity to the stranger mouse, versus an empty cage. In contrast, “two-hit” mice failed to show sociability, as they spent significantly less time in proximity to the stranger mouse than all three other groups.

The subsequent test for social novelty preference required mice to discriminate between stranger 1 and a newly introduced mouse (stranger 2; Fig. 4B). In this more complex social test, the vehicle group had significant preference for novel stranger 2, while all three of the other treatment groups failed to demonstrate this shift in preference.

The changes in social preference could not be attributed to low exploration in the treated groups. In fact, during the sociability test (Fig. 4C), the “two-hit” mice made significantly more entries into the empty cage side than all three other treatment groups. No significant effects of treatment or side were observed for entries during the test for social novelty preference (Fig. 4D).

3.2.2. Impaired spatial learning in Morris water maze in mice at 7.5 months following LPS or “two-hit” treatments—PD is primarily a movement disorder that can eventually result in memory abnormalities and dementia in about 50% of the patients (Caballol et al., 2007). The memory function of these treated mice was measured by using Morris water maze (MWM) test. Before one year of age, no effects of treatment were observed on swimming ability in a visible platform test, or latencies to escape during a 5-day training period in a hidden platform test (Fig. 5A–B). Following acquisition, mice were given a one-minute probe test with the platform removed. As shown in Fig. 5C, mice treated with either vehicle or DSP-4 alone spent significantly more percent time in the target quadrant, where the platform had been located. In contrast, mice exposed to LPS or “two-hit” failed to demonstrate quadrant selectivity. A significant effect of quadrant was also found for crossings of the platform and corresponding locations; however, within-treatment group tests indicated that the LPS alone group and “two-hit” mice failed to demonstrate a preference for swimming across the previous location of the platform (Fig. 5D). Since swimming speed did not differ between the groups (Supplementary Table 1), the learning deficits in the probe test were not due to deficits in swimming ability. In addition, all groups of mice demonstrated a high degree of proficiency in the visual cue task.

3.2.3. “Two-hit” mice display progressive bowel disorders—Constipation is among the most common non-motor symptoms of PD (Ashraf et al., 1997). It is usually

defined as the occurrence of dry, hard and/or small stools, infrequent stools, stools that are difficult to expel, or sensation of incomplete evacuation. Although one-hour stool collection results revealed stool frequency to be altered in both DSP-4 alone and LPS alone mice, with a decrease in frequency at 3 months after treatment (Fig. 6A), the ratio of dry weight to wet weight of feces did not show any difference when compared with control (Fig. 6B). Of interest, we found that DSP-4 not only significantly attenuated LPS-induced stool frequency, but it clearly caused an increase of dry/wet feces ratio at 6 and 10 months after LPS injection (Fig. 6A and B), indicating severe defecatory dysfunction.

3.2.4. "Two-hit" mice display exaggerated startle response and PPI—

The sensorimotor gating of auditory startle response (ASR) is a brainstem reflex elicited by an unexpected acoustic stimulus. It is reported that PD patients show greater ASR than control subjects (Nieuwenhuijzen et al., 2006), we therefore measured the prepulse inhibition (PPI) of the ASR in those mice. The results showed that the "two-hit" mice demonstrated exaggerated startle responses (Fig. 7A) and PPI (Fig. 7B) at 74 dB at 10 months after injection, in comparison to the age-matched LPS group. No significant group differences were found between mice exposed to DSP-4 alone, LPS alone, and vehicle. Overall, these results suggest that the combined DSP-4 and LPS challenge led to hyper-reactivity to acoustic stimuli.

3.3. DSP-4 treatment accelerates the appearance of non-motor symptoms in LPS-treated mice: Phenotypes in older mice (12 to 21 months of age)

In our second study, mice were given a first treatment (vehicle or DSP-4) at 9-14 weeks of age, and a second treatment (vehicle or LPS) one week later. Mice were tested in the elevated plus maze at either 10.5 or 17.5 months after DSP-4/LPS injection, and the buried food assay at either 11 or 18.5 months after DSP-4/LPS injection. The results showed that "two-hit" mice had significant deficits in both tests, but only at an older age.

3.3.1. "Two-hit" mice display anxiety phenotype at 17.5 months after injection—

NE is widely recognized as playing a role in anxiety disorder, which are reported with a high prevalence in PD patients (Walsh and Bennett, 2001). In the present study, anxiety-like behavior was measured using the elevated plus maze. The treatments had no significant effects on anxiety-like behavior at 10.5 months after DSP-4/LPS injection (data not shown). Mice in all treatment conditions spent a comparable time exploring the open arms. However, 17.5 months following the DSP-4/LPS injections, differences were observed between the treatment groups (Fig. 8). A repeated measures ANOVA on time spent on each arm indicated that, while the first treatment (either DSP-4 or vehicle) had ni significant effects in its own, there was a significant interaction between the second treatment (either LPS or vehicle) and arm of the maze (the repeated measure) [$F(1,30)=5.02$, $p=0.0327$] (Fig. 8A). Post-hoc analyses revealed that the "two-hit" mice, given both DSP-4 and LPS, spent less time on the open arms, and more time in the closed arms, than the Vehicle/Vehicle or DSP-4/Vehicle groups. Further, the "two-hit" mice made significantly fewer entries into the open arms than the vehicle-treated mice (Fig. 8B).

3.3.2. "Two-hit" mice display olfactory discrimination deficits at 18.5 months after injection—Olfactory dysfunction is one of the earliest manifestations of PD, which has been found in nearly all PD patients (Doty, 2012; Hawkes et al., 1997). However, in our study, mice showed generally good performance across treatment conditions, with 100% of the group finding the buried food at 11 months after DSP-4/LPS injections (Fig. 9). However, at 18.5 months after DSP-4/LPS injections, the "two-hit" mice had significantly longer latencies to find the buried food than the vehicle-treated mice. Further, two of the older mice failed to locate the buried food: one from the DSP-4 alone group and one from the "two-hit" group.

Altogether, our findings suggest that the "two-hit" mice displayed a series of Parkinsonian-like nonmotor symptoms.

3.4. DSP-4 treatment time-dependently accelerates appearance of motor symptoms in LPS-treated mice

To determine whether DSP-4 treatment could accelerate the onset or aggravate the severity of motor dysfunction in LPS-treated mice, we measured a variety of motor activities, including rotarod test, wire hang test, and gait tests.

3.4.1. "Two-hit" mice display a progressive reduction in rotarod ability—The rotarod test was used to evaluate the motor coordination of animals. No changes in rotarod performance were observed until 6 months after treatments, but only "two-hit" mice showed a decreased latency to fall from the rotarod, in comparison to the vehicle, DSP-4 alone, and LPS alone group (Fig. 10A). Compared with age-matched vehicle controls, the performance in rotarod was significantly reduced in both DSP-4 alone and LPS alone group 10 months after treatment, whilst DSP-4 further potentiated the LPS-induced motor deficits.

3.4.2. "Two-hit" mice display a progressive reduction in wire hang performance—With wire hanging tests, balance, coordination, and muscle condition can be assessed. These tests are based on the knowledge that mice are eager to remain hanging on a wire or grid till exhaustion. A significant reduction in wire hang performance was observed only in "two-hit" mice and LPS-injected mice at 3 months after treatments, DSP-4 markedly accelerated the onset of the motor dysfunction and the severity was enhanced by LPS treatment at 6 months (Fig. 10B). However, no obvious changes in wire hang performance was found in the mice treated with DSP-4 alone, LPS alone, and "two-hit" groups 10 months after treatments.

3.4.3. "Two-hit" mice display severe gait disorders—Gait disturbance is one of the cardinal symptoms in patients with PD. We used DigiGait imaging system to quantify posture and kinematics of these mice. "Two-hit" mice clearly showed severe gait disturbance 10 months after treatments, characterized by increasing paw angle to keep balance (Fig. 10C) and increasing brake time to compensate for instability (Fig. 10D) compared to age-matched vehicle, DSP-4 alone, and LPS alone mice in all behavioral testing sessions. Moreover, the unforced moving gait analysis system also showed shorter mean stride lengths

variability (Fig. 10E, F), duck flippers feet, dragging steps, and twisted walking track (Fig. 10E, G) in “two-hit” mice 10 months after treatments.

Altogether, our findings suggest that DSP-4 accelerates appearance of motor symptoms in LPS-treated mice.

4. Discussion

In this study, we demonstrated that dysfunction of the brain norepinephrine system by DSP-4 accelerated the appearance of several behavioral deficits and exacerbated neurotoxicity in LPS-injected mouse PD model. Mechanistic studies revealed that the synergistic effects of this “two-hit” mouse PD model is associated with earlier activation of microglia and aggravated oxidative injuries on brain regions innervated by LC/NE neurons and thus, leading to earlier neurodegeneration. Consequently, distinct motor deficits and nonmotor function abnormities were observed at different stages of disease progression in mice treated with DSP-4/LPS. Together, our results demonstrated that this “two-hit” mouse PD model approximates the pathogenesis and clinical symptoms of PD patients and can be a suitable tool for further mechanistic study and development of potential therapeutic interventions.

4.1. Advantages of “Two-hit model”

Recent reports from our laboratory demonstrate that chronic neuroinflammation in mice may approximate this ascending degenerative pattern (Song et al., 2018). We found that a single systemic injection of LPS or DSP-4 initiated chronic neuroinflammation and produced a time-dependent ascending degenerative pattern in mouse brain: neurodegeneration afflicts noradrenergic neurons of the locus coeruleus three months before progressing to dopaminergic neurons of the SNpc and six months before progressing into neurons of the primary motor cortex and hippocampus. These two rodent models have been valuable for studying the pathogenesis of PD. However, mice injected with LPS or DSP-4 requires 6-12 months to display significant neuron loss and motor function deficits. The time-consuming aspect has become a practical concern for routine uses of either LPS or DSP-4 alone as a rodent PD model. The “two-hit” model has successfully rectified this time issue; as accelerated appearance of PD-related pathologies was observed. Mice injected with DSP-4/LPS displayed progressive motor deficits in rotarod (show a decreased trend but no statistic difference) and wire hang performance beginning at 3 months after treatments, advancing at 6 months, and remaining unchanged at 10 months that appears to correlate with the loss of SN/DA neurons (Fig. 10). Moreover, gait disturbances, a commonly observed motor symptom in PD patients which is characterized by increased paw angle to keep balance and prolonged brake time to compensate for instability were detected only in “two-hit” mice, but not mice injected alone either with DSP-4 or LPS (Fig. 10 C–D). Together, accelerated and more pronounced changes of these motor deficits illustrate the advantage of using this “two-hit” model in PD study.

Furthermore, the numbers of striatal and VTA neurons in “two-hit”, DSP-4- and LPS-injected mice were not significantly different from than that of age-matched control mice. These findings are in line with other reports found in PD patients: 1) despite clear presence

of dendritic degeneration, nonsignificant changes of numbers of medium spiny neurons were found in PD patients (Zaja-Milatovic et al., 2005); 2) despite the selective, progressive loss of DA neurons in the SNpc, the very similar DA neurons in the VTA demonstrate a higher degree of resistance to degeneration (Brichta and Greengard, 2014; Dauer and Przedborski, 2003). Regarding to the unchanged striatal neurons in our “two-hit”, DSP-4-, or LPS-injected mice, one possibility is that CPu receives little noradrenergic innervation, while other affected brain regions, such as hippocampus, cortex and midbrain, are heavily innervated by noradrenergic nerve fibers (Robertson et al., 2013; Uematsu et al., 2015). In addition to LPS or DSP-4, the neuronal loss is also unchanged in VTA in MPTP-injected mice (Brichta and Greengard, 2014). It has been reported that VTA neurons express much higher levels of calbindin-D28K, a Ca^{2+} buffering protein, in comparison to SNpc neurons (Fu et al., 2012). The majority of VTA neurons and a small percentage of SNpc neurons with expressing high levels of this Ca^{2+} buffering protein are spared from neurodegeneration in PD(Rcom-H’cheo-Gauthier et al., 2014; Yamada et al., 1990).

Previous research in PD has focused mainly on the DA system in the nigrostriatal cells as the key cause of motor dysfunction. A substantial number of individuals with PD exhibit debilitating non-motor symptoms, such as affective disorders, sensory impairment, and cognitive decline (Braak et al., 2003; Hawkes et al., 2010; Langston, 2006; Poewe, 2008). The cause of the non-motor symptoms associated with PD is currently under intense investigation. Accumulating evidence suggests a central role of brain NE in modulating some of these non-motor symptoms (Delaville et al., 2011; Devauges and Sara, 1991; Lauterbach, 1993; Mather and Harley, 2016). NE/LC neurons innervate most brain regions and play pivotal roles in modulating the reactivity of many neural circuits mediating a variety of behavioral and physiological responses. Our “two-hit” model provides a valuable opportunity to study changes of PD-related non-motor functions. Indeed, a series of premotor/motor behaviors deficits were observed at early stages in DSP-4/LPS mice: 1) Although at a later stage, only the “two-hit” mice showed significant olfactory abnormality to find the buried food and anxiety behavior with increase in the percentage closed arm time in the elevated plus maze 16 months after treatment, which are reported with a high association with PD patients; 2) Only the “two-hit” mice failed to show significant sociability 3 months after treatments, and spent less time in proximity to the stranger mouse than all 3 other groups; 3) The “two-hit” mice exhibit severe disturbances in GI function in comparison to the age-matched DSP-4 alone and LPS alone groups, characterized by decreased stool frequency and altered dry/wet feces ratio that increases with age; 4) Only the “two-hit” mice demonstrated a significant exaggerated startle response and prepulse inhibition at 10 months compared to that produced by DSP-4 or LPS alone, suggesting marked sensorimotor gating impairment; 5) Mice exposed to LPS or “two-hit” failed to demonstrate quadrant selectivity at 8 months, then mice in all 3 treated groups showed a comparable impaired spatial learning in the MWM at 10 months. The ASR is one of the most widely studied psychophysiological measures in the cognitive and affective sciences. The ASR to an unexpected loud stimulus is regarded as a brainstem reflex originating in the nucleus reticularis pontis caudalis and being distributed up the brainstem and down the spinal cord along slowly conducting pathways (Kofler et al., 2001). It is notable that similar increases in startle amplitude and prepulse inhibition have been reported in the MitoPark

mouse model for PD (Grauer et al., 2014). It has been reported that the integrity of the LC-NE system plays a key role in memory encoding (Lemon et al., 2009) and in determining late-life cognitive abilities (Mather and Harley, 2016); Novelty detection is accompanied by increased hippocampal NA activity, driven by enhanced firing of the LC (Kitchigina et al., 1997; Sara et al., 1994); LC stimulation improves memory retrieval (Devauges and Sara, 1991), whereas vagus nerve stimulation enhances memory encoding and consolidation via LC activation (Clark et al., 1999; Ghacibeh et al., 2006). In our study, no further memory loss was observed in the "two-hit" mice after 10 months. One possibility is that there is no further LC-TH positive neurons and hippocampal neuronal loss at that time point.

Taken together, results from this "two-hit model provide strong evidence confirming the crucial role of low-grade chronic inflammation in producing PD-like caudal-rostral degeneration and associated behavioral changes. In addition, the unique time-dependent neurodegeneration in different brain regions, plus motor/nonmotor behavioral changes after LPS or DSP-4 give credence that this "two-hit" regimen offers an excellent rodent PD model for screening potential disease modifying drugs.

4.2. Mechanism of actions

It is interesting to note that despite difference in chemical structure, LPS and DSP-4 produce similar patterns of neuroinflammation, oxidative stress-related injuries and neuronal loss in various regions of mouse brain. Our previous studies indicate that prolonged increase in the production of superoxide/ROS is essential for maintaining chronic neuroinflammation in both LPS and DSP-4 models (Song et al., 2018). Chronic neuroinflammation leads to enhanced oxidative and nitrosylative injuries that dictate the temporal order of degeneration observed among different susceptible neuronal populations. Inhibiting NOX2, the key enzyme involved in inflammation-mediated production of superoxide, successfully suppressed chronic neuroinflammation and prevented oxidative neuronal injuries and neurodegeneration following LPS/DSP-4 injection. Comparisons of how these two toxins activate microglia and the subsequent evolvement of brain inflammation may offer insights into the mechanism of inflammation-related neurodegeneration. Although LPS cannot cross the blood-brain barrier (BBB), our previously studies have shown that pro-inflammatory factors, such as TNFα (Qin et al., 2013; Qin et al., 2007), produced in the periphery after systemic LPS administration, are transported through BBB. Once in brain, these factors activate microglia, leading to the synthesis of additional pro-inflammatory factors, creating a persistent and self-propelling neuroinflammation that drives delayed and progressive loss of neurons in brain. By contrast, DSP-4 is capable of crossing BBB and depleting brain NE by directly damaging NE/LC neurons, and causes sustained microglial activation (Jiang et al., 2015). LPS is known to directly activate microglia to trigger acute immune responses in the brain. If acute phase of inflammation is not properly resolved, brain immune system may turn into protracted low-grade chronic neuroinflammation and produce progressive neurodegeneration (Qin et al., 2013; Qin et al., 2007). By contrast, DSP-4 does not directly activate microglia (Jiang et al., 2015). Several reports indicate that DSP-4, through the depletion of NE by damaging NE/LC neurons, indirectly causes microglial activation. In fact, activation of microglia was not initially observed within the first few days after DSP-4 injection. It is intriguing to observe that once the microglia were activated around 2 weeks

after DSP-4 injection, persistent activation of microglia and low-grade chronic neuroinflammation was continually observed in all LC-NE innervated brain regions, even up to 10 months following the DSP-4 injection. Thus, DSP-4 model serves as a good example showing that acute immune responses may not always be necessary for the formation of chronic brain inflammation. We speculate that the microglial activation and persistent chronic neuroinflammation elicited by DSP-4 injection are likely due to the occurrence of reactive microgliosis through the action of danger-associated molecular pattern (DAMP) released from damaged terminals of NE/LC neurons. We have previously reported that DAMP-associated reactive microgliosis is a critical immune response in maintaining chronic neuroinflammation vicious cycle and leading to progressive neurodegeneration (Chen et al., 2016). It is worth noting that although LPS and DSP-4 produce chronic brain inflammation through different mechanisms, it appears that once low-grade chronic inflammation develops and becomes persistent, both toxins have very similar patterns of pathologies. Furthermore, the different mode of action of LPS and DSP-4 in causing brain inflammation offers a pharmacological explanation for the synergistic actions both in neurodegeneration and behavioral deficits seen mice injected with these two toxins.

4.3. Discuss literature related to DSP-4 followed by LPS by other groups

Low-grade, chronic inflammation has been associated with many neurodegenerative diseases, but the mechanisms responsible for producing this inflammation remain unclear. It is generally believed that aging is an important factor in neurodegenerative diseases. Nevertheless, most of the reported studies have used either acute or sub-chronic animal PD models, which did not offer a sufficient time window for observing the progressive neuron loss and behavioral changes. A general pattern immerged from our previous reports indicating that as long as chronic neuroinflammation persists for a certain period, neuronal loss and behavioral dysfunction eventually follow. However, most of the reports did not document the neurodegeneration.

Interestingly, a similar study was conducted in rats by Iravani et al. produced different results (Iravani et al., 2014). Their results suggested that a single intraperitoneal dose of DSP-4 administered 8 days previously, caused a marked loss of TH positive neurons in LC but no change in DA cell number in SN. Moreover, following combined DSP-4 treatment, LPS-induced nigral DA neuronal loss failed to be exacerbated by the loss of LC-NA input. One critical factor for the apparent inability of DSP-4 to induce SN/DA neuronal loss or exacerbate LPS-induced SN/DA neuronal loss in their study is timing. In our study, 1) rather than 8 days, it takes up to 6 months for mice to show about only 15% SN/DA neuron loss after DSP-4 alone treatment; 2) they employed intranigral administration of LPS, which could cause acute and severe (50% loss of TH-ir neurons) SN/DA neurodegeneration within few days; while intraperitoneal injection with LPS requires up to 10 months for disease progression to achieve −50% SN/DA neuronal loss in our study. It’s important to note that, in our study, the loss of TH-ir neurons in SN following by DSP-4 alone, LPS alone, or even their combined challenge was not significantly different when it comes to 10 months of treatments, suggesting a ceiling effect on the SN/DA neuronal loss in response to DSP-4/LPS challenge.

5. Conclusion

Taken together, this study demonstrated a significant benefit of combining NE depletion with chronic neuroinflammation for recapitulating PD-like features in mouse, which was characterized by progressive loss of neurons in a caudo-rostral pattern associates with the appearance of non-motor/motor symptoms and, most importantly, shortened the time to disease progression. Our findings also contribute with new knowledge about how LC damage affects their innervated brain regions. This “two-hit” mouse model for the first time shows the temporal detail of disease progression and indicates targeting microglia activation as a disease-modifying strategy for PD may shed new light on PD, which could provide invaluable for the development of treatments that can alleviate non-motor/motor symptoms and stop progressive neurodegeneration through interaction with affected neurotransmissions system, particularly those that occur at early stages of the disease.

Supplementary Material

Refer to Web version on PubMed Central for supplementary material.

Acknowledgments

This research was supported through the Intramural Research Program at the National Institute of Environmental Health Sciences (NIEHS) to J.S. Hong in the National Institutes of Health (NIH), USA; National Institute of Mental Health (R01MH111429) and National Institute of Neurological Disorders and Stroke (R01NS091236) to Y.Y.I. Shih. We thank Dr. Ling-Wan Chen from Biostatistics & Computational Biology Branch, NIEHS/NIH, for assistance with statistical analysis; we thank Anthony Lockhart for assistance with animal colony management and maintenance.

Reference

Ashraf W, Pfeiffer RF, Park F, Lof J, Quigley EM, 1997 Constipation in Parkinson’s disease: objective assessment and response to psyllium. Movement disorders : official journal of the Movement Disorder Society 12, 946–951. [PubMed: 9399219]

Block ML, Zecca L, Hong JS, 2007 Microglia-mediated neurotoxicity: uncovering the molecular mechanisms. Nature reviews. Neuroscience 8, 57–69. [PubMed: 17180163]

Braak H, Del Tredici K, Rub U, de Vos RA, Jansen Steur EN, Braak E, 2003 Staging of brain pathology related to sporadic Parkinson’s disease. Neurobiology of aging 24, 197–211. [PubMed: 12498954]

Braak H, Ghebremedhin E, Rub U, Bratzke H, Del Tredici K, 2004 Stages in the development of Parkinson’s disease-related pathology. Cell and tissue research 318, 121–134. [PubMed: 15338272]

Braak H, Thal DR, Del Tredici K, 2011 Nerve cells immunoreactive for p62 in select hypothalamic and brainstem nuclei of controls and Parkinson’s disease cases. Journal of neural transmission 118, 809–819. [PubMed: 21052746]

Brichta L, Greengard P, 2014 Molecular determinants of selective dopaminergic vulnerability in Parkinson’s disease: an update. Front Neuroanat 8, 152. [PubMed: 25565977]

Caballol N, Marti MJ, Tolosa E, 2007 Cognitive dysfunction and dementia in Parkinson disease. Movement disorders : official journal of the Movement Disorder Society 22 Suppl 17, S358–366. [PubMed: 18175397]

Cai Z, Chattopadhyay N, Liu WJ, Chan C, Pignol JP, Reilly RM, 2011 Optimized digital counting colonies of clonogenic assays using ImageJ software and customized macros: comparison with manual counting. Int J Radiat Biol 87, 1135–1146. [PubMed: 21913819]

Chen SH, Oyarzabal EA, Hong JS, 2016 Critical role of the Mac1/NOX2 pathway in mediating reactive microgliosis-generated chronic neuroinflammation and progressive neurodegeneration. Curr Opin Pharmacol 26, 54–60. [PubMed: 26498406]

Clark KB, Naritoku DK, Smith DC, Browning RA, Jensen RA, 1999 Enhanced recognition memory following vagus nerve stimulation in human subjects. Nature neuroscience 2, 94–98. [PubMed: 10195186]

Dauer W, Przedborski S, 2003 Parkinson's disease: mechanisms and models. Neuron 39, 889–909. [PubMed: 12971891]

Delaville C, Deurwaerdere PD, Benazzouz A, 2011 Noradrenaline and Parkinson's disease. Front Syst Neurosci 5, 31. [PubMed: 21647359]

Devauges V, Sara SJ, 1991 Memory retrieval enhancement by locus coeruleus stimulation: evidence for mediation by beta-receptors. Behavioural brain research 43, 93–97. [PubMed: 1650233]

Dias V, Junn E, Mouradian MM, 2013 The role of oxidative stress in Parkinson's disease. Journal of Parkinson's disease 3, 461–491.

Dickson DW, Braak H, Duda JE, Duyckaerts C, Gasser T, Halliday GM, Hardy J, Leverenz JB, Del Tredici K, Wszolek ZK, Litvan I, 2009 Neuropathological assessment of Parkinson's disease: refining the diagnostic criteria. The Lancet. Neurology 8, 1150–1157. [PubMed: 19909913]

Doty RL, 2012 Olfactory dysfunction in Parkinson disease. Nat Rev Neurol 8, 329–339. [PubMed: 22584158]

Fearnley JM, Lees AJ, 1991 Ageing and Parkinson's disease: substantia nigra regional selectivity. Brain : a journal of neurology 114 (Pt 5), 2283–2301. [PubMed: 1933245]

Fritschy JM, Grzanna R, 1989 Immunohistochemical analysis of the neurotoxic effects of DSP-4 identifies two populations of noradrenergic axon terminals. Neuroscience 30, 181–197. [PubMed: 2747911]

Fu Y, Yuan Y, Halliday G, Rusznak Z, Watson C, Paxinos G, 2012 A cytoarchitectonic and chemoarchitectonic analysis of the dopamine cell groups in the substantia nigra, ventral tegmental area, and retrorubral field in the mouse. Brain Struct Funct 217, 591–612. [PubMed: 21935672]

Gassmann M, Grenacher B, Rohde B, Vogel J, 2009 Quantifying Western blots: pitfalls of densitometry. Electrophoresis 30, 1845–1855. [PubMed: 19517440]

Ghacibeh GA, Shenker JI, Shenal B, Uthman BM, Heilman KM, 2006 The influence of vagus nerve stimulation on memory. Cognitive and behavioral neurology : official journal of the Society for Behavioral and Cognitive Neurology 19, 119–122. [PubMed: 16957488]

Grauer SM, Hodgson R, Hyde LA, 2014 MitoPark mice, an animal model of Parkinson's disease, show enhanced prepulse inhibition of acoustic startle and no loss of gating in response to the adenosine A(2A) antagonist SCH 412348. Psychopharmacology 231, 1325–1337. [PubMed: 24150248]

Hawkes CH, Del Tredici K, Braak H, 2010 A timeline for Parkinson's disease. Parkinsonism Relat D 16, 79–84.

Hawkes CH, Shephard BC, Daniel SE, 1997 Olfactory dysfunction in Parkinson's disease. J Neurol Neurosurg Psychiatry 62, 436–446. [PubMed: 9153598]

Hoehn MM, Yahr MD, 1967 Parkinsonism: onset, progression and mortality. Neurology 17, 427–442. [PubMed: 6067254]

Iravani MM, Sadeghian M, Rose S, Jenner P, 2014 Loss of locus coeruleus noradrenergic neurons alters the inflammatory response to LPS in substantia nigra but does not affect nigral cell loss. Journal of neural transmission 121, 1493–1505. [PubMed: 24781752]

Jiang L, Chen SH, Chu CH, Wang SJ, Oyarzabal E, Wilson B, Sanders V, Xie K, Wang Q, Hong JS, 2015 A novel role of microglial NADPH oxidase in mediating extra-synaptic function of norepinephrine in regulating brain immune homeostasis. Glia 63, 1057–1072. [PubMed: 25740080]

Jonsson G, Hallman H, Ponzio F, Ross S, 1981 DSP4 (N-(2-chloroethyl)-N-ethyl-2-bromobenzylamine)--a useful denervation tool for central and peripheral noradrenaline neurons. European journal of pharmacology 72, 173–188. [PubMed: 6265244]

Kitchigina V, Vankov A, Harley C, Sara SJ, 1997 Novelty-elicited, noradrenaline-dependent enhancement of excitability in the dentate gyrus. The European journal of neuroscience 9, 41–47. [PubMed: 9042567]

Kofler M, Muller J, Wenning GK, Reggiani L, Hollosi P, Bosch S, Ransmayr G, Valls-Sole J, Poewe W, 2001 The auditory startle reaction in parkinsonian disorders. Movement disorders : official journal of the Movement Disorder Society 16, 62–71. [PubMed: 11215594]

Langston JW, 2006 The Parkinson's complex: parkinsonism is just the tip of the iceberg. Annals of neurology 59, 591–596. [PubMed: 16566021]

Lauterbach EC, 1993 The locus ceruleus and anxiety disorders in demented and nondemented familial parkinsonism. Am J Psychiatry 150, 994.

Lemon N, Aydin-Abidin S, Funke K, Manahan-Vaughan D, 2009 Locus coeruleus activation facilitates memory encoding and induces hippocampal LTD that depends on beta-adrenergic receptor activation. Cerebral cortex 19, 2827–2837. [PubMed: 19435710]

Li Q, Li L, Fei X, Zhang Y, Qi C, Hua S, Gong F, Fang M, 2018 Inhibition of autophagy with 3-methyladenine is protective in a lethal model of murine endotoxemia and polymicrobial sepsis. Innate Immun 24, 231–239. [PubMed: 29673286]

Li ZS, Schmauss C, Cuenca A, Ratcliffe E, Gershon MD, 2006 Physiological modulation of intestinal motility by enteric dopaminergic neurons and the D2 receptor: analysis of dopamine receptor expression, location, development, and function in wild-type and knock-out mice. The Journal of neuroscience : the official journal of the Society for Neuroscience 26, 2798–2807. [PubMed: 16525059]

Litvan I, Bhatia KP, Burn DJ, Goetz CG, Lang AE, McKeith I, Quinn N, Sethi KD, Shults C, Wenning GK, Movement Disorders Society Scientific Issues, C., 2003 Movement Disorders Society Scientific Issues Committee report: SIC Task Force appraisal of clinical diagnostic criteria for Parkinsonian disorders. Movement disorders : official journal of the Movement Disorder Society 18, 467–486. [PubMed: 12722160]

Mather M, Harley CW, 2016 The Locus Coeruleus: Essential for Maintaining Cognitive Function and the Aging Brain. Trends in cognitive sciences 20, 214–226. [PubMed: 26895736]

Niehaus I, Lange JH, 2003 Endotoxin: is it an environmental factor in the cause of Parkinson's disease? Occup Environ Med 60, 378.

Nieuwenhuijzen PH, Horstink MW, Bloem BR, Duysens J, 2006 Startle responses in Parkinson patients during human gait. Experimental brain research 171, 215–224. [PubMed: 16307244]

Olanow CW, Tatton WG, 1999 Etiology and pathogenesis of Parkinson's disease. Annual review of neuroscience 22, 123–144.

Poewe W, 2008 Non-motor symptoms in Parkinson's disease. European journal of neurology 15 Suppl 1 14–20. [PubMed: 18353132]

Qin L, Liu Y, Hong JS, Crews FT, 2013 NADPH oxidase and aging drive microglial activation, oxidative stress, and dopaminergic neurodegeneration following systemic LPS administration. Glia 61, 855–868. [PubMed: 23536230]

Qin L, Wu X, Block ML, Liu Y, Breese GR, Hong JS, Knapp DJ, Crews FT, 2007 Systemic LPS causes chronic neuroinflammation and progressive neurodegeneration. Glia 55, 453–462. [PubMed: 17203472]

Rcom-H'cheo-Gauthier A, Goodwin J, Pountney DL, 2014 Interactions between calcium and alpha-synuclein in neurodegeneration. Biomolecules 4, 795–811. [PubMed: 25256602]

Richard IH, McDermott MP, Kurlan R, Lyness JM, Como PG, Pearson N, Factor SA, Juncos J, Serrano Ramos C, Brodsky M, Manning C, Marsh L, Shulman L, Fernandez HH, Black KJ, Panisset M, Christine CW, Jiang W, Singer C, Horn S, Pfeiffer R, Rottenberg D, Slevin J, Elmer L, Press D, Hyson HC, McDonald W, Group S.-P.S., 2012 A randomized, double-blind, placebo-controlled trial of antidepressants in Parkinson disease. Neurology 78, 1229–1236. [PubMed: 22496199]

Robertson SD, Plummer NW, de Marchena J, Jensen P, 2013 Developmental origins of central norepinephrine neuron diversity. Nature neuroscience 16, 1016–1023. [PubMed: 23852112]

Rommelfanger KS, Edwards GL, Freeman KG, Liles LC, Miller GW, Weinshenker D, 2007 Norepinephrine loss produces more profound motor deficits than MPTP treatment in mice. P Natl Acad Sci USA 104, 13804–13809.

Ross SB, Renyl AL, 1976 On the long-lasting inhibitory effect of N-(2-chloroethyl)-N-ethyl-2-bromobenzylamine (DSP 4) on the active uptake of noradrenaline. The Journal of pharmacy and pharmacology 28, 458–459. [PubMed: 6763]

Sara SJ, Vankov A, Herve A, 1994 Locus coeruleus-evoked responses in behaving rats: a clue to the role of noradrenaline in memory. Brain research bulletin 35, 457–465. [PubMed: 7859103]

Song S, Jiang L, Oyarzabal EA, Wilson B, Li Z, Shih YI, Wang Q, Hong JS, 2018 Loss of Brain Norepinephrine Elicits Neuroinflammation-Mediated Oxidative Injury and Selective Caudo-Rostral Neurodegeneration. Mol Neurobiol.

Uematsu A, Tan BZ, Johansen JP, 2015 Projection specificity in heterogeneous locus coeruleus cell populations: implications for learning and memory. Learn Mem 22, 444–451. [PubMed: 26330494]

Walsh K, Bennett G, 2001 Parkinson's disease and anxiety. Postgrad Med J 77, 89–93. [PubMed: 11161073]

Wang Q, Chu CH, Qian L, Chen SH, Wilson B, Oyarzabal E, Jiang L, Ali S, Robinson B, Kim HC, Hong JS, 2014 Substance P exacerbates dopaminergic neurodegeneration through neurokinin-1 receptor-independent activation of microglial NADPH oxidase. The Journal of neuroscience : the official journal of the Society for Neuroscience 34, 12490–12503. [PubMed: 25209287]

Wang Q, Qian L, Chen SH, Chu CH, Wilson B, Oyarzabal E, Ali S, Robinson B, Rao D, Hong JS, 2015 Post-treatment with an ultra-low dose of NADPH oxidase inhibitor diphenyleneiodonium attenuates disease progression in multiple Parkinson's disease models. Brain : a journal of neurology 138, 1247–1262. [PubMed: 25716193]

Yamada T, McGeer PL, Baimbridge KG, McGeer EG, 1990 Relative sparing in Parkinson's disease of substantia nigra dopamine neurons containing calbindin-D28K. Brain research 526, 303–307. [PubMed: 2257487]

Zaja-Milatovic S, Milatovic D, Schantz AM, Zhang J, Montine KS, Samii A, Deutch AY, Montine TJ, 2005 Dendritic degeneration in neostriatal medium spiny neurons in Parkinson disease. Neurology 64, 545–547. [PubMed: 15699393]

Zarow C, Lyness SA, Mortimer JA, Chui HC, 2003 Neuronal loss is greater in the locus coeruleus than nucleus basalis and substantia nigra in Alzheimer and Parkinson diseases. Archives of neurology 60, 337–341. [PubMed: 12633144]

Highlights:

- Depletion of norepinephrine (NE) accelerates LPS-induced sequential loss of neurons
- DSP-4 potentiates LPS-induced microglial activation in LC-innervated brain regions
- DSP-4 potentiates LPS-induced neuronal oxidative stress in brain
- “Two-hit” mice display Parkinson-like nonmotor symptoms
- NE depletion accelerates appearance of motor symptoms in LPS-treated mice

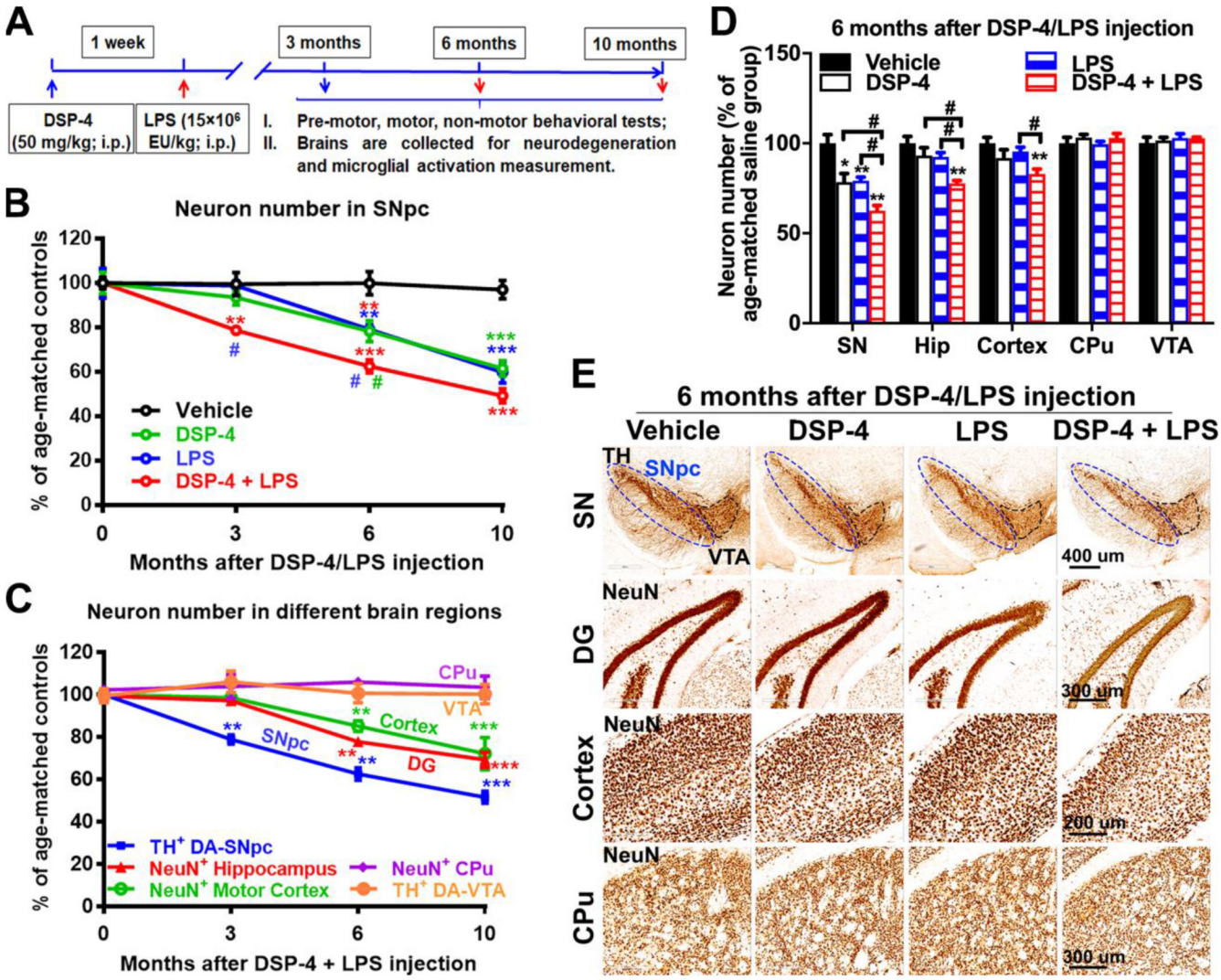

Fig. 1. DSP-4 treatment accelerates neurodegeneration in LPS-treated mice brain.

(A) Schematic drawing of the treatment regimen for DSP-4 and LPS. Male C57BL/6J mice received a single injection of DSP-4 (50 mg/kg, i.p.), followed by LPS (15×10^6 EU/kg, i.p.) treatment one week later. 3, 6 and 10 months after LPS injection, mice were sacrificed for immunohistological staining of different brain regions. (B) DSP-4 accelerates SN-DA neurodegeneration in LPS-treated mouse brains [two-way ANOVA, treatment x time interaction, $F(9,50)=5.525$, $p<0.0001$; effect of time, $F(3,50)=49.93$, $p<0.0001$; effect of treatment, $F(3,50)=28.36$, $p<0.0001$], $^{*}p<0.05$, $^{**}p<0.01$, $^{***}p<0.001$ compare with age-matched vehicle controls. $^{\#}p<0.05$ compare with age-matched DSP-4- (green) or LPS- (blue) treated animals. (C) Quantitative analysis of neuron loss in the different brain regions at different time points after "two-hit" treatment. TH-immunoreactive neurons in both SNpc and VTA were counted stereologically. Neurons in hippocampal granule layer (Neu-N-immunoreactive), motor cortex and CPu (Neu-N-immunoreactive) were quantified by auto-counting using ImageJ software. Results are expressed as a percentage of age-matched vehicle controls (mean ± SEM) in each group at each time point [one-way ANOVA for each region with time as main effect, SNpc: $F(3,11)=55.07$, $p<0.0001$; Hippocampus:

F(3,9)=31.93, p<0.0001; Motor cortex: F(3,19)=8.938, p=0.0007; CPu: F(3,17)=0.2363, p=0.8698; VTA: F(3, 4)=0.3179, p=0.8123], $^{**}p<0.01$, $^{***}p<0.001$ compare with age-matched vehicle controls. (D) Quantitative analysis of neuron loss in different brain regions at 6 months after DSP-4, LPS, or “two-hit” treatment. Hip=Hippocampus. Results are expressed as a percentage of age-matched vehicle controls (mean ± SEM) from 4-5 mice in each group at each time point [two-way ANOVA, treatment x brain region interaction, F(9,89)=3.364, p=0.0014; effect of treatment, F(3,89)=9.949, p<0.0001; effect of brain region, F(3,89)=20.4, p<0.0001]. $^{*}p<0.05$ and $^{**}p<0.01$ compare with age-matched vehicle controls. $^{\#}p<0.05$ compare with indicated groups. (E) Representative images of staining in SN, hippocampus, motor cortex, and CPu at 6 months after injection were shown. Dopaminergic neurons in the SNpc were stained with anti-TH antibody. Neurons in hippocampal granule layer, motor cortex and CPu were stained with anti-Neu-N antibody. Scales as indicated in the pictures.

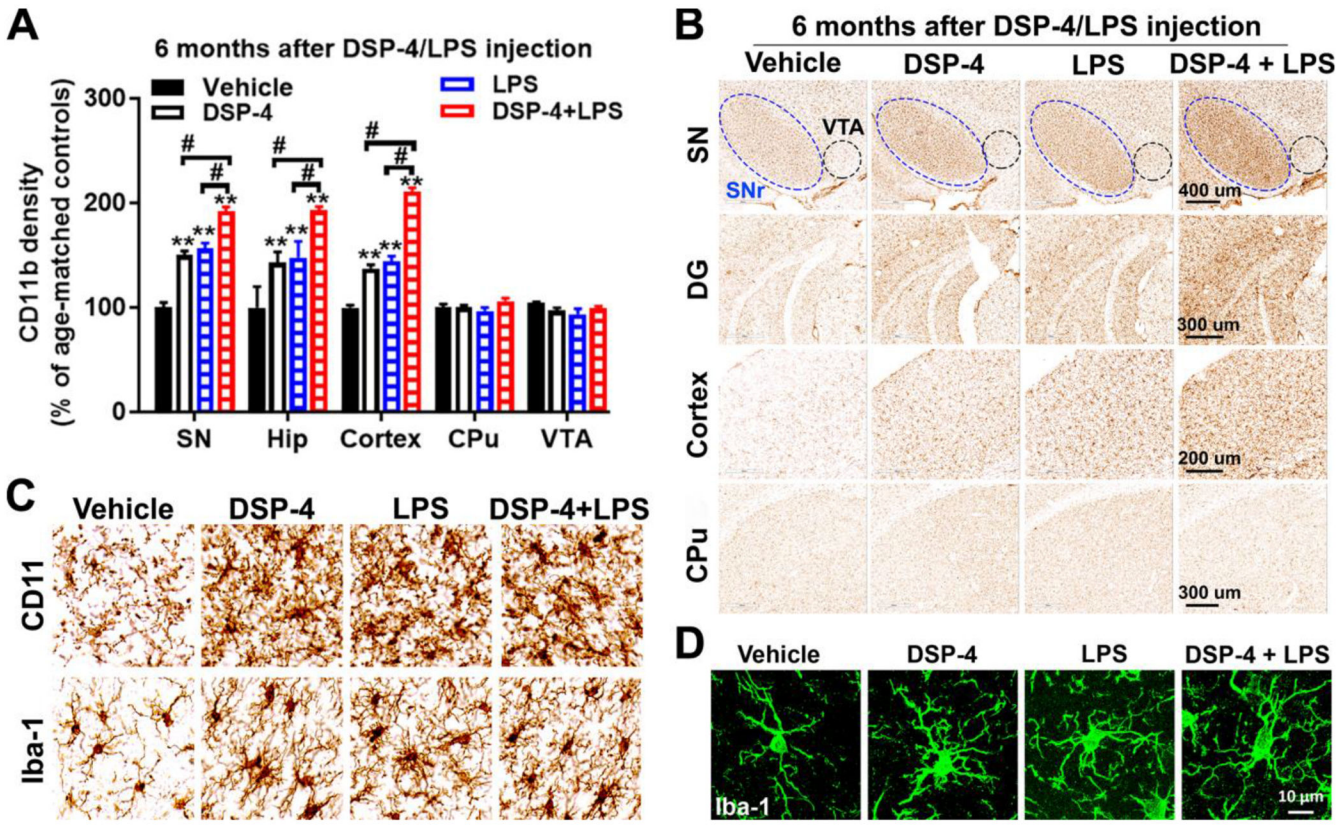

Fig. 2. DSP-4 treatment potentiates microglial activation in LPS-treated mice.

Male C57BL/6J mice received a single injection of DSP-4 (50 mg/kg, i.p.), followed by LPS (15×10^6 EU/kg, i.p.) treatment one week later. 3, 6 and 10 months following the LPS injection, microglia in SN, VTA, hippocampus, motor cortex and CPu were stained with CD11b antibodies. (A) Quantitative analysis of microglial activation in these brain regions at 6 months after injection by measuring alterations of CD11b density [two-way ANOVA, treatment x brain region interaction, $F(12,109)=12.4$, $p=0.0014$; effect of treatment, $F(4,109)=69.91$, $p<0.0001$; effect of brain region, $F(4,109)=66.77$, $p<0.0001$]. $^{**}p<0.01$ compare with age-matched vehicle controls. $^{\#}p<0.05$ compare with indicated groups. (B) Representative images of CD11b staining in different brain regions at 6 months after injection were shown. Scales as indicated in the pictures. (C-D) High-power images show the morphological changes in microglia and an increase in microglial CD11b and Iba-1 in SN at 6 months after DSP-4/LPS injection.

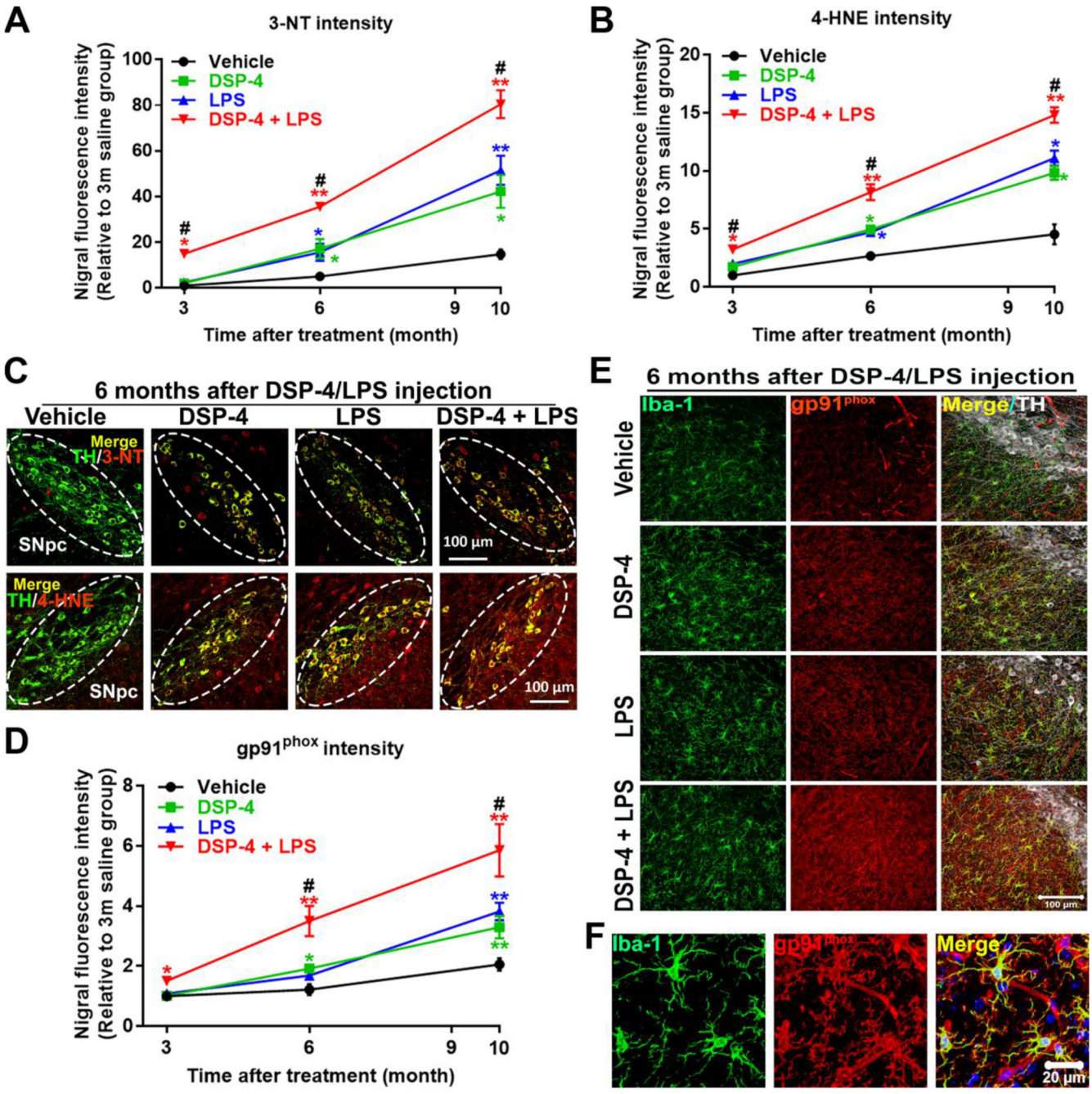

Fig. 3. DSP-4 treatment potentiates neuronal oxidative stress in LPS-treated mice.

Male C57BL/6J mice received a single injection of DSP-4 (50 mg/kg, i.p.), followed by LPS (15×10^6 EU/kg, i.p.) treatment one week later. 3, 6 and 10 months following the LPS injection, oxidative damage in protein and in lipid in SN were stained with anti-3-NT or anti-4-HNE antibody. (A-B) The fluorescence intensity of 3-NT [two-way ANOVA, treatment x time interaction, F(6,101)=11.28, p<0.0001; effect of treatment, F(3,101)=54.13, p<0.0001; effect of time, F(2,101)= 178.1, *p*<0.000l] (A) and 4-HNE [two-way ANOVA, treatment x time interaction, F(6,88)=11.1, *p*<0.0001; effect of treatment, F(3,88)=65.31,

p<0.0001; effect of time, F(2,88)=212.2, p<0.0001] (B) in the SN was quantified. (C) Representative images show double labeled TH and 3-NT (top) and TH and 4-HNE (bottom) in SN 6 months after LPS injection. Images were captured at 40× magnification. The SNpc zone is outlined in white dots. (D) The fluorescence intensity of $gp91^{phox}$ in the SN was quantified [two-way ANOVA, treatment x time interaction, F(6,90)=2.382, p=0.035; effect of treatment, F(3,90)=10.11, p<0.0001; effect of time, F(2,90)=42.03, p<0.0001]. (E) SN were triple labeled for $gp91^{phox}$, Iba-1 and TH. Images were captured at 40× magnification. (F) The high-power images to show co-localization of Iba-1 and $gp91^{phox}$ in SN. The selected SN area was confirmed by TH (white) staining. Results are expressed as a percentage of age-matched vehicle controls (mean ± SEM). *p<0.05, **p<0.01 compare with age-matched vehicle controls. $^{\#}p$<0.05 compare with age-matched DSP-4 and LPS alone groups. Scales as indicated in the pictures.

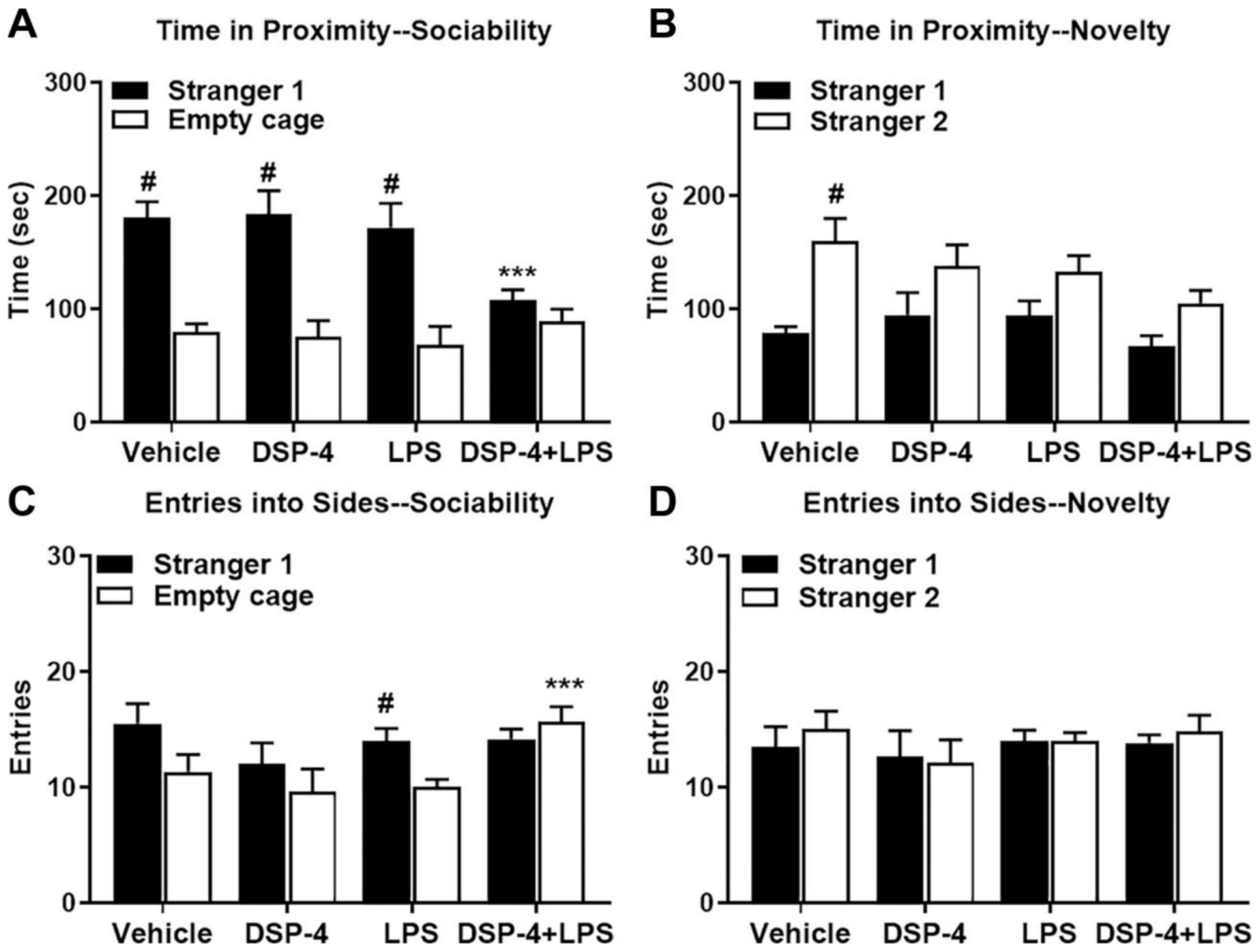

Fig. 4. Loss of sociability in "two-hit" mice.

Male C57BL/6J were tested at **3.5 months after exposed to DSP-4/LPS**. (A) "Two-hit" mice failed to show sociability, as they spent a comparable time with stranger mouse and empty cage, but significantly less time in proximity to the stranger mouse than all three other groups, [within-group analyses following repeated measures ANOVA, treatment x side interaction, $F(3,20)=3.39$, $p=0.0381$; and effect of side, $F(1,20)=49.97$, $p<0.0001$], (B) Mice failed to show social novelty preference in the all toxins-treated groups, [main effect of treatment, $F(3,20)=3.61$, $p=0.0313$; and side, $F(1,20)=16.57$, $p=0.0006$]. (C) "Two-hit" mice made significantly more entries into the empty cage side than all three other treatment groups, [treatment x side interaction, $F(3,20)=5.09$, $p=0.0089$; effect of side, $F(1,20)=14.85$, $p=0.001$]. (D) No significant effects of treatment or side were observed for entries during the test for social novelty preference. Data are mean (± SEM) for 10-min tests. N=6 mice per treatment group. #$p<0.05$, within-treatment group comparison to opposite side. ***$p<0.05$, comparison to all three other groups with the same colored bar.

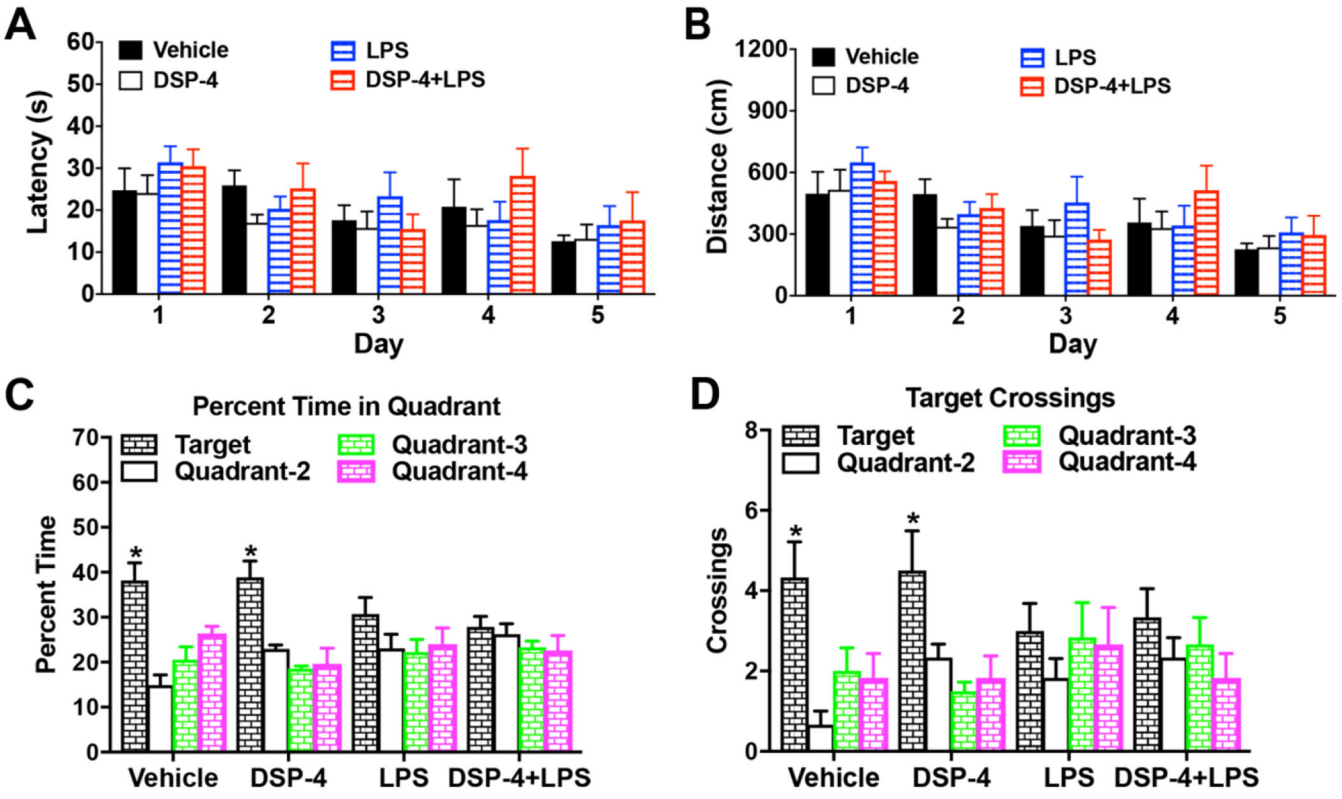

Fig. 5. "Two-hit" and LPS-injected mice display Impaired spatial learning in Morris water maze at 7.5 months after injection.

Mice were 42 weeks in age at time of testing, following treatment with DSP-4 and/or LPS at 9-10 weeks. **(A-B)** Acquisition of spatial learning in the Morris water maze. Data are means (± SEM) of 4 trials per day, across 5 days of training. **(A)** Latency to find the escape platform in the Morris water maze. **(B)** Swimming distance. **(C-D)** The decrease in spending percent time, [within-group analyses following repeated measures ANOVA, treatment x quadrant interaction, $F(9,60)=2.06$, $p=0.0473$; and quadrant, $F(3,60)=13.51$, $p<0.0001$] **(C)** and crossing times, [effect of quadrant, $F(3,60)=7.80$, $p=0.0002$;] **(D)** in target quadrant in LPS alone and "two-hit" mice. Data are means (± SEM) for a one-minute probe trial, with the escape platform removed from the water maze. The target quadrant indicates the location of the platform during training. N=6 mice per treatment group. *$p<0.05$, significant effect of quadrant, within-treatment repeated measures ANOVA.

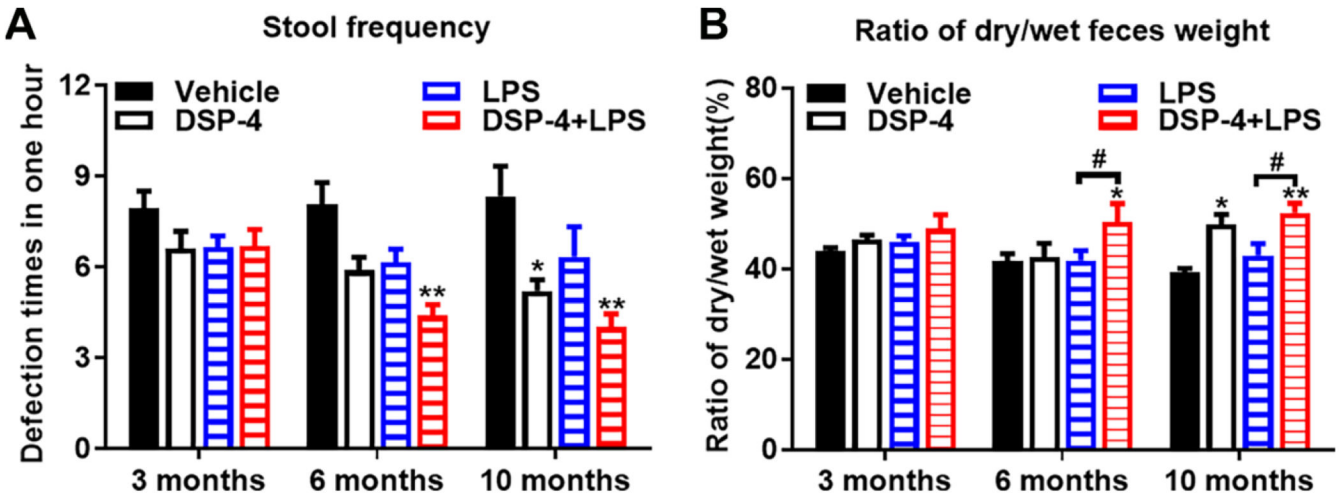

Fig. 6. Mice suffers from chronic constipation after exposed to both DSP-4 and LPS.

Male C57BL/6J mice received a single injection of DSP-4 (50 mg/kg, i.p.), followed by LPS (15×10^6 EU/kg, i.p.) treatment one week later. (A) "two-hit" mice exhibited decreased defecation frequency compared with age-matched control animals at 6 and 10 months, [effect of treatment, $F(3,127)=11.76$, $p<0.0001$]. (B) The ratios of dry weight and wet weight of feces were measured as an indication of constipation, [effect of treatment, $F(3,138)=6.179$, $p=0.0006$]. Results represent average defecation frequency for two trials ± SEM for 9 animals per group. *$p< 0.05$, **$p< 0.01$ compare with age-matched vehicle controls. $^{\#}p< 0.05$ compare with LPS-alone group.

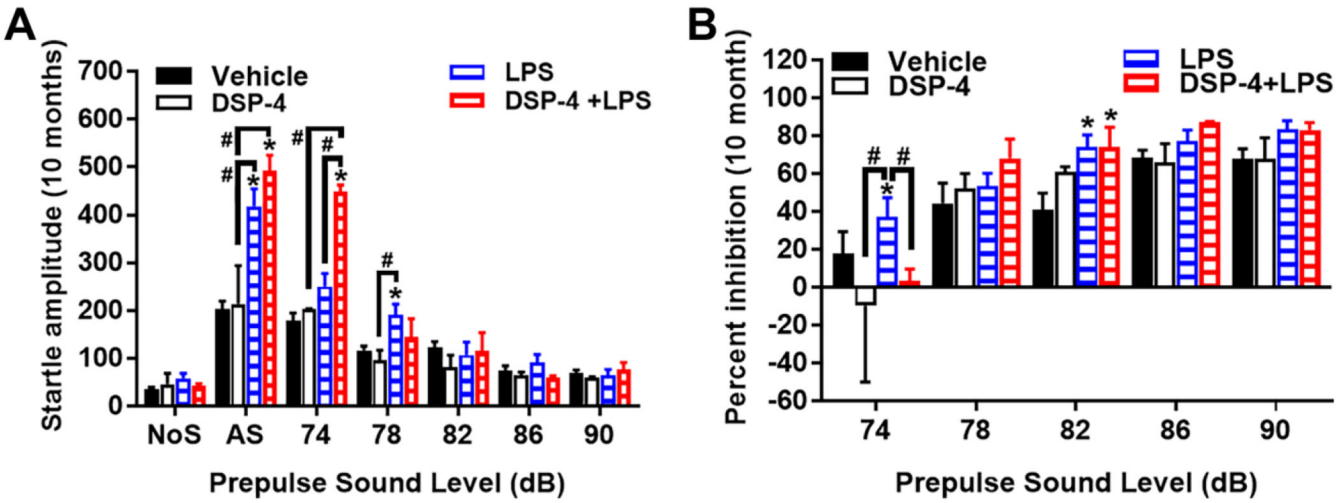

Fig. 7. "Two-hit" mice display exaggerated startle response and PPI.

Increased acoustic startle response, [repeated measures ANOVA, treatment x decibel level interactions, $F(12,96)=2.09$, $p=0.0249$] **(A)** and percentage PPI, [repeated measures ANOVA, treatment x decibel level interactions, $F(8,64)=2.51$, $p=0.0195$] **(B)** in male C57BL/6J mice at 10 months after DSP-4/LPS injection. Data shown are means (± SEM) for each group. Trials included no stimulus (NoS) trials and acoustic startle stimulus (AS; 120 dB) alone trials. $^{*}p<0.05$, comparison to vehicle group. $^{\#}p< 0.05$ compare with indicated group.

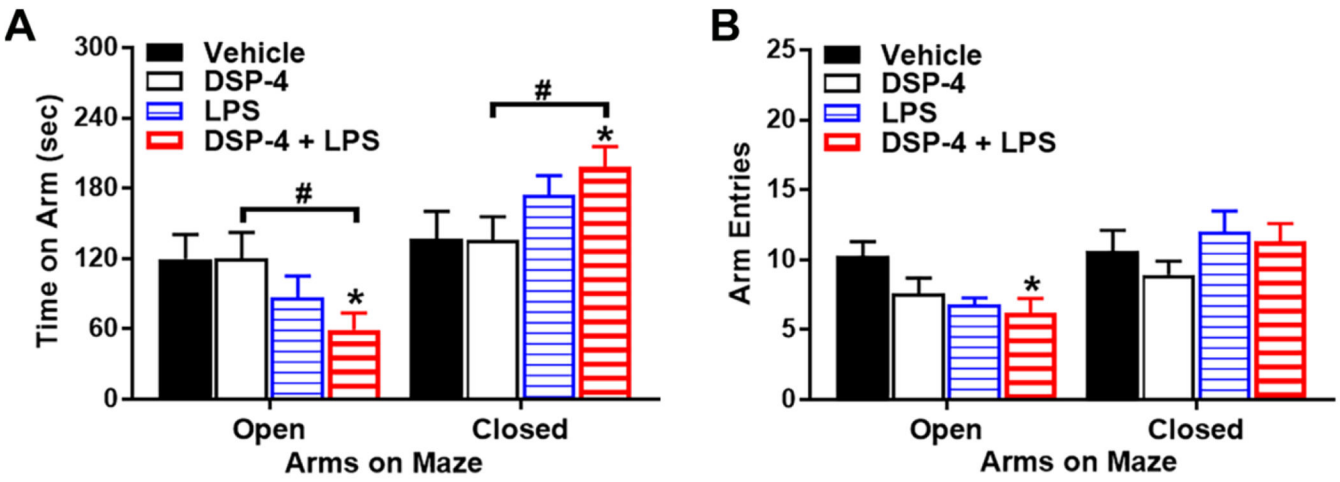

Fig. 8. Anxiety-like behavior on an elevated plus maze.

Male C57BL/6J mice were tested at 17.5 months after injection with DSP-4/LPS. **(A)** "Two-hit" mice spent less time on the open arms, and more time in the closed arms, than the Vehicle or DSP-4 groups, [repeated measures ANOVA, second treatment (LPS) x maze arm interactions, $[F(1,30)=5.02, p=0.0327]$, **(B)** "Two-hit" mice made significantly fewer entries into the open arms than the vehicle-treated mice, [second treatment x maze arm interaction, $F(1,30)=10.68, p=0.0027]$, N=5-12 mice per treatment group. *$p<0.05$, comparison to Vehicle. #$p<0.05$, comparison to DSP-4.

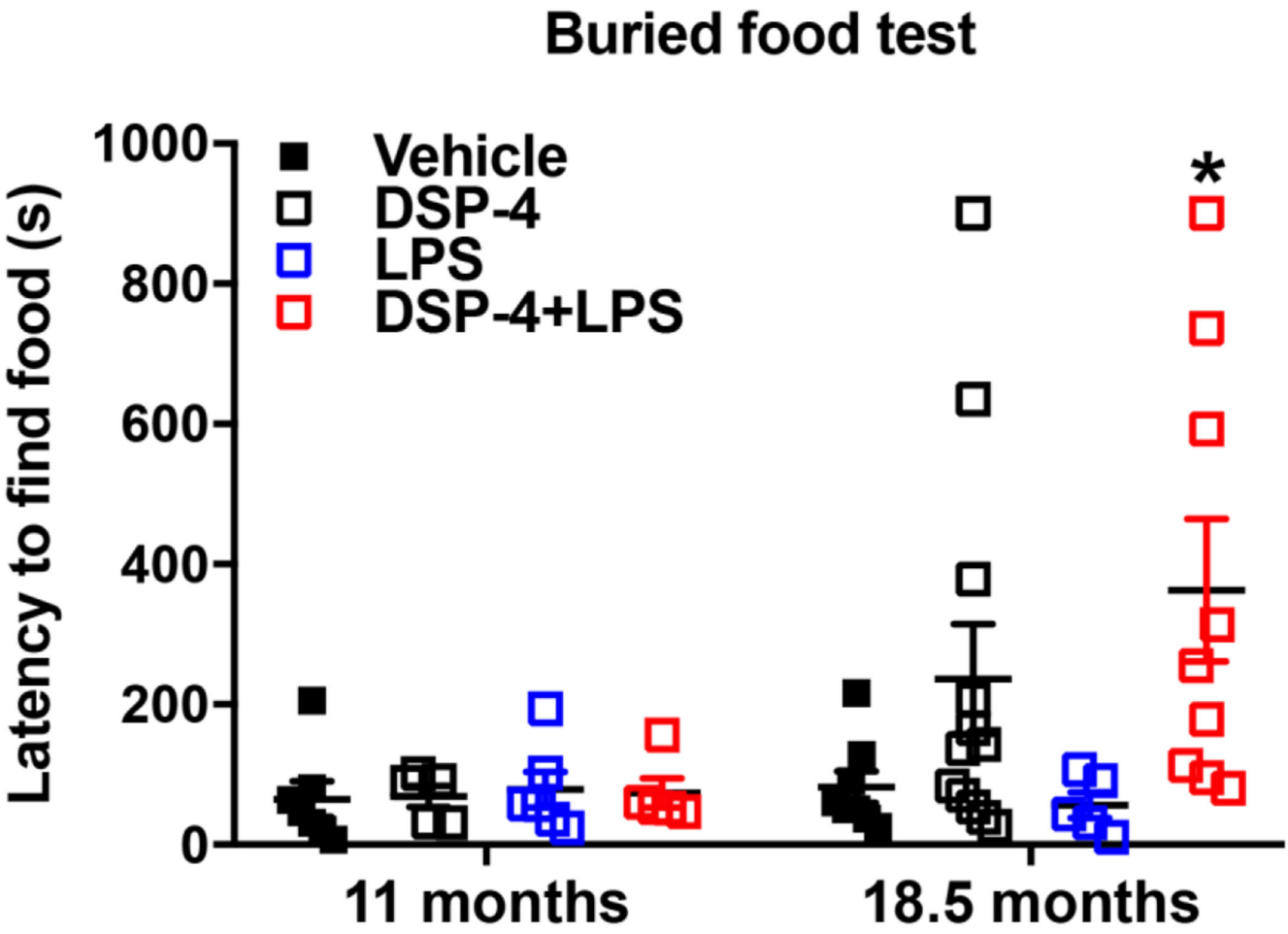

Fig. 9. Latencies (sec) in a buried food test for olfactory ability.

Male C57BL/6J mice were tested at 11 or 18.5 months after injection with DSP-4/LPS. In the older mice, combined treatment with DSP-4 and LPS led to significantly longer latencies to locate the buried food, [F(1,30)=7.72, p=0.0093], N=5-7 mice per treatment group at 11 months, and 5-12 mice per treatment group at 18.5 months after injections. *p<0.05, comparison to Vehicle.

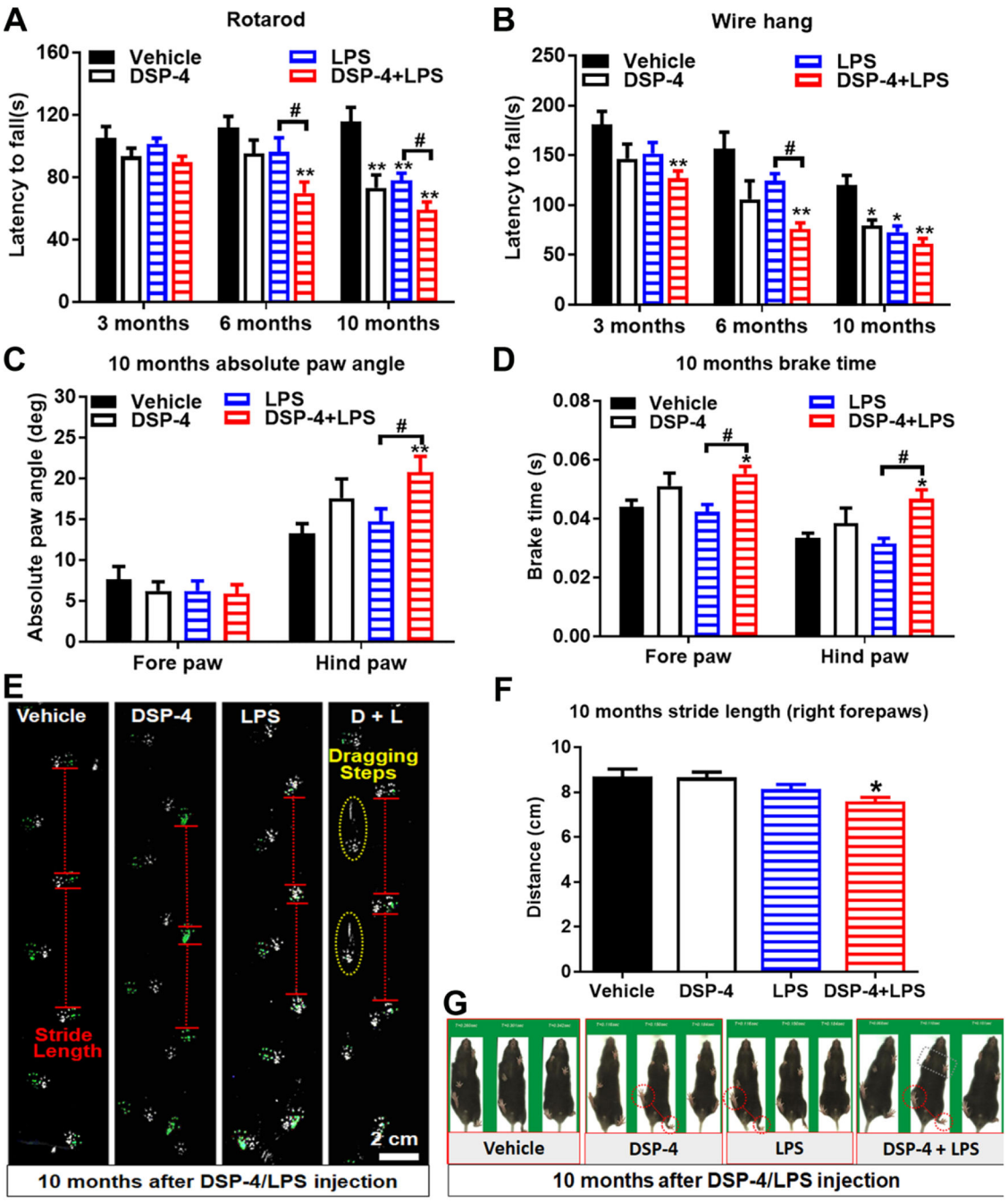

Fig. 10. DSP-4 treatment accelerates appearance of motor symptoms in LPS-treated mice.

Male C57BL/6J mice received a single injection of DSP-4 (50 mg/kg, i.p.), followed by LPS (15×10^6 EU/kg, i.p.) treatment one week later. 3, 6 and 10 months following LPS injection, corresponding motor behaviors were tested. (A) Examination of motor function by the rotarod test. Time spent balanced on top of the rotating rod (latency) was measured across six test trials for indicated treated mice. Significant differences between “two-hit” mice and LPS-treated mice were observed. Two-way ANOVA, treatment x time interaction, $F(6,111)=1.996$, $p=0.0722$; effect of time, $F(2,111)=9.836$, $p=0.0001$; effect of treatment,

F(3,111)=12.07, p<0.0001. (B) Wire hang test. Error bars are expressed as means ± SEM, n=8-10. Two-way ANOVA, treatment x time interaction, F(6,113)=0.9446, p=0.4662; effect of time, F(2,113)=16.22, p<0.0001; effect of treatment, F(3,113)=8.646, p<0.0001. (C-D) Examination of absolute paw angle, [treatment x paw interaction, F(3,71)=3.5, p=0.0198; effect of paw, F(1,71)=74.53, p<0.0001] (C) and brake time, [effect of paw, F(1,66)=23.2, p<0.0001; effect of treatment, F(3,66)=9.361, p<0.0001] (D) in gait analysis by using DigiGait system. Data were analyzed by two-way ANOVA. Error bars are expressed as means ± SEM, n=8-10. *p<0.05, **p<0.01 compare with age-matched vehicle controls. $^{\#}p$<0.05 compare with LPS-alone group. The unforced moving gait analysis system also showed shorter mean stride lengths variability, [F: one-way ANOVA, F(3,21)=4.227, p=0.0174] (E-G), duck flippers feet (E and G), dragging steps (E), and twisted walking track (E and G) in the “two-hit” mice 10 months after treatments.